Electronic Supplementary Material (ESI) for Soft Matter.

Supporting Information for

Strategies for Promoting Discotic Nematic Phases

Carson O. Zellman[1] and Vance E. Williams[1]

[1]Department of Chemistry, Simon Fraser University, Burnaby, BC V5A 1S6, Canada

vancew@sfu.ca

Table of Contents

1. Synthesis and Identification

1.1. Materials and Instrumentation

Materials. Dry dichloromethane (CH_2Cl_2; anhydrous, ≥99.8%, contains 40−150 ppm amylene as a stabilizer, Sigma Aldrich, Oakville, ON, Canada) was used as the solvent for reactions employing CH_2Cl_2. All other solvents used for syntheses and workups were reagent grade and were used as received without further purification. The following reagents employed for all syntheses were used as received: glacial acetic acid (99.7%, ACP, Montréal, QC), 4-dimethylaminopyridine (DMAP; >99.0%, Tokyo Chemical Industry Co., Portland, OR, USA), and 1-ethyl-3-(3-dimethylaminopropyl)carbodiimide (EDC; Oakwood Chemical, Estill, SC, USA). Column chromatography was performed using Silicycle Ultrapure silica gels 2500 (Parc-Technologique, 40-63 μm (230−400 mesh), Quebec City, QC, Canada). Drying of the organic extracts was performed using magnesium sulfate ($MgSO_4$; BDH, reagent grade, Radnor, PA). The nuclear magnetic resonance (NMR) solvent $CDCl_3$ (D 99.8%, Cambridge Isotope Laboratories, Andover, MA) was used as received.

Instrumentation. All instrumentation measurements were performed at Simon Fraser University (SFU), Burnaby, BC, Canada, unless stated otherwise. The 400 MHz ^{1}H-NMR spectra were obtained on a Bruker AVANCE III 400 MHz NMR spectrometer with a 5 mm BBOF probe. The 600 MHz ^{1}H-NMR, COSY, HSQC, HMBC, and 150 MHz ^{13}C-NMR spectra were obtained on a Bruker AVANCE II 600 MHz spectrometer equipped with a 5 mm QNP cryoprobe and an Ultrashield 600 Plus magnet. For the S2 2-D HMBC ^{1}H-^{13}C correlation spectra, the pulse sequence (hmbcgplpndgf) used 1 ms sine-shaped gradient pulses (ratio 50:30:40.1) for selection and was optimized for long-range (2- and 3-bond) couplings. A low pass J-filter was used to suppress one-bond correlations. No decoupling was applied during acquisition. A total of 256 increments were acquired with 8 scans per increment, 16 dummy scans, and a recycle delay of 1.5 s. The 1/(^{2}J)CH delay was set to 3.45 ms (^{1}J(CH) = 145 Hz), a 62.5 ms delay was used for evolution of long-range couplings (^{2,3}J(CH) = 8 Hz), and a 200 μs homospoil/gradient recovery delay was used.

Mass spectrometry (MS) measurements were performed using a microOTOF-Q II instrument (Bruker, direct electrospray ionization (ESI), scan range: 50−3000 *m*/*z*, set capillary at 4500 V, end plate

offset at -500 V, 0.3 bar nebulizer, 180 °C dry heater, dry gas injected at 4.0 L/min, University of Notre Dame Mass Spectrometry and Proteomics Facility). Some compounds could not be obtained by direct ESI. In these cases, matrix-assisted laser desorption/ionization (MALDI) equipped with a time-of-flight (TOF) mass spectrometer (MALDI-TOF) was used (Bruker UltrafleXtreme MALDI-TOF-TOF, scan range: 50 m/z to 3500 m/z, University of Notre Dame Mass Spectrometry and Proteomics Facility). MS data of **DBP-OH(10)** was obtained on an ultra-high resolution quadrupole instrument (Bruker maxis impact, ESI, TOF MS, scan range: 50−2000 *m*/*z*, Mass Spectrometry Services, SFU).

1.2. Synthesis

The following precursors were synthesized according to previously reported methods: the phenanthrene quinone **Q(10)**: 2,3,6,7-tetrakis(decyloxy)phenanthrene-9,10-dione;[1] 3,4-diaminophenol, **DBP-A(6,OHx)**: 2,3,6,7,12-pentakis(hexyloxy)dibenzo[a,c]phenazine-11-carboxylic acid, and **DBP-OH(6)**: 2,3,6,7-tetrakis(hexyloxy)dibenzo[a,c]phenazine-11-ol;[2] **DBP-A(6)**: 2,3,6,7-tetrakis(hexyloxy)dibenzo[a,c]phenazine-11-carboxylic acid and **DBP-A(10)**: 2,3,6,7-tetrakis(decyloxy)dibenzo[a,c]phenazine-11-carboxylic acid.[3]

2,3,6,7-Tetrakis(decyloxy)dibenzo[a,c]phenazine-11-ol (DBP-OH(10)). In a round bottom flask (100 mL) equipped with a magnetic stir bar, **Q(10)** (440 mg, 0.53 mmol) and freshly made 3,4-diaminophenol (~410 mg) were stirred in anhydrous ethanol (80 mL). Glacial acetic acid (10 drops) was added, and the dark red-purple mixture was refluxed over 3 days. The resulting red-brown mixture was cooled to room temperature, poured over ice (200 g), and stirred for 30 min. The solid product was then collected by vacuum filtration, washed copiously with distilled water, ethanol, and acetone, in sequence, air dried and put under vacuum for 3 hours, yielding a dark yellow powder (418.8 mg, 85%). The compound was too insoluble to obtain NMR data. HRMS (ESI^+ of $M + H^+$): m/z for $C_{60}H_{92}N_2O_5$: calculated: 921.7084; experimental: 921.7079.

2,3,6,7-Tetrakis(hexyloxy)dibenzo[a,c]phenazine-11-yl 2,3,6,7-tetrakis(hexyloxy)dibenzo[a,c]phenazine-11-carboxylate (dDBP(6,6)). A flame dried, three-neck round bottom flask (50 mL) equipped with a magnetic stir bar under a nitrogen atmosphere was charged with dry CH_2Cl_2 (20 mL). The solvent was purged with nitrogen and **DBP-OH(6)** (67.1 mg, 0.0963 mmol) was added, and the mixture was stirred at room temperature for 5 min. To the dark yellow-brown mixture was added: **DBP-A(6)** (140.6 mg, 0.1939 mmol) and 4-dimethylaminopyridine (DMAP) (71.8 mg, 0.588 mmol), in sequence. The yellow-brown suspension was stirred at 0 °C for 20 min. At this time, 1-ethyl-3-(3-dimethylaminopropyl carbodiimide (EDC) (138.0 mg, 0.7199 mmol) was added and the yellow-brown mixture was stirred at ambient temperature for 15 hours. The resulting dark orange-brown mixture was diluted with CH_2Cl_2 (50 mL) and subsequently washed with H_2O (3 * 25 mL), 10% v/v HCl (25 mL), and brine (25 mL), dried over $MgSO_4$ and concentrated on a rotary evaporator to afford a yellow-brown solid. The crude product was purified by column chromatography using a gradient of 90–100% CH_2Cl_2 in hexanes as the eluent (L = 15.0 cm, R_f = 0.19–0.54). The compound was further purified *via* recrystallization from EtOH in CH_2Cl_2, yielding a bright orange powder (51.5 mg, 38%). ^{1}H NMR ($CDCl_3$, 400 MHz): δ 9.23 (d, 1H, *J* = 1.6 Hz), 8.70 (s, 1H), 8.692 (s, 1H), 8.690 (s, 1H), 8.66 (s, 1H), 8.54 (dd, 1H, *J* = 8.9, 1.9 Hz), 8.37 (d, 1H, *J* = 9.0 Hz), 8.35 (d, 1H, *J* = 9.4 Hz), 8.27 (d, 1H, *J* = 2.5 Hz), 7.78 (dd, 1H, *J* = 9.1, 2.6 Hz), 7.641 (s, 1H), 7.639 (s, 1H), 7.637 (s, 1H), 7.63 (s, 1H), 4.35 (t, 2H, *J* = 6.5 Hz), 4.338 (m, 2H), 4.336 (t, 2H, *J* = 6.3 Hz), 4.33 (t, 2H, *J* = 6.5 Hz), 4.28 (t, 2H, *J* = 6.7 Hz), 4.27 (t, 2H, *J* = 6.4 Hz), 4.264 (t, 2H, *J* = 6.8 Hz), 4.257 (t, 2H, *J* = 6.6 Hz), 1.99 (m, 16H), 1.62 (m, 16H), 1.43 (m, 32H), 0.970 (t, 3H, *J* = 6.9 Hz), 0.967 (t, 3H, *J* = 6.8 Hz), 0.962 (t, 3H, *J* = 7.3 Hz), 0.959 (t, 3H, *J* = 7.0 Hz), 0.956 (t, 3H, *J* = 6.9 Hz), 0.95 (m, 6H), 0.94 (t, 3H, *J* = 7.0 Hz) ppm. ^{13}C{^{1}H} NMR ($CDCl_3$, 150 MHz): δ 164.9, 152.4, 152.1, 151.9, 151.7, 149.5, 149.40, 149.39, 149.34, 143.8, 143.5, 142.9, 142.2, 141.8, 141.7, 140.5, 139.8, 133.3, 130.4, 129.8, 129.0, 128.3, 127.3, 126.7, 126.6, 126.5, 124.6, 123.7, 123.5, 123.33, 123.28, 120.1, 108.9, 108.6, 108.5, 106.2, 106.13, 106.08, 106.07, 106.05, 69.63, 69.62, 69.59, 69.58, 69.18, 69.15, 69.12, 31.89, 31.88, 31.87, 31.86, 29.53, 29.49, 29.47, 29.44, 29.43, 26.044, 26.041, 26.03, 26.02, 26.01, 26.000, 25.997, 22.862, 22.859, 22.840, 22.836, 22.83, 14.269, 14.267, 14.26, 14.244, 14.241, 14.239 ppm (15 carbon signals missing or overlapping). HRMS (ESI$^+$ of M + H$^+$): m/z for $C_{89}H_{118}N_4O_{10}$: calculated: 1403.8921; experimental: 1403.8908.

2,3,6,7-Tetrakis(decyloxy)dibenzo[a,c]phenazine-11-yl 2,3,6,7-tetrakis(hexyloxy)dibenzo[a,c]phenazine-11-carboxylate (dDBP(6,10)). A flame dried, three-neck round bottom flask (50 mL) equipped with a magnetic stir bar under a nitrogen atmosphere was charged with dry CH_2Cl_2 (20 mL). The solvent was purged with nitrogen and **DBP-OH(10)** (69.3 mg, 0.0752 mmol), **DBP-A(6)** (55.9 mg, 0.0771 mmol), and DMAP (29.6 mg, 0.242 mmol) were added, in sequence. The dark yellow suspension was stirred at 0 °C for 20 min. At this time, EDC (54.0 mg, 0.282 mmol) was added, and the dark yellow mixture was stirred at ambient temperature for 20 hours. The resulting yellow-brown mixture was diluted with CH_2Cl_2 (25 mL) and subsequently washed with H_2O (3 * 25 mL), 10% v/v HCl (25 mL), and brine (25 mL), dried over $MgSO_4$ and concentrated on a rotary evaporator to afford an orange-brown solid. The crude product was purified by column chromatography using a gradient of 80−100% CH_2Cl_2 in hexanes as the eluent (L = 11.8 cm, R_f = 0.21−0.57). The compound was further purified *via* recrystallization from ethyl acetate, yielding an orange powder (66.0 mg, 54%). ^{1}H NMR ($CDCl_3$, 400 MHz): δ 9.21 (d, 1H, *J* = 1.9 Hz), 8.67 (s, 1H), 8.66 (s, 1H), 8.65 (s, 1H), 8.62 (s, 1H), 8.53 (dd, 1H, *J* = 8.9, 1.9 Hz), 8.35 (d, 1H, *J* = 8.6 Hz), 8.33 (d, 1H, *J* = 8.9 Hz), 8.25 (d, 1H, *J* = 2.5 Hz), 7.77 (dd, 1H, *J* = 9.1, 2.6 Hz), 7.62 (s, 1H), 7.61 (s, 2H), 7.59 (s, 1H), 4.35 (t, 2H, *J* = 6.6 Hz), 4.33 (t, 4H, *J* = 6.7 Hz), 4.32 (t, 2H, *J* = 6.7 Hz), 4.28 (t, 2H, *J* = 6.5 Hz), 4.27 (t, 2H, *J* = 6.3 Hz), 4.25 (t, 2H, *J* = 6.4 Hz), 4.24 (t, 2H, *J* = 6.7 Hz), 1.99 (m, 16H), 1.62 (m, 16H), 1.44 (m, 32H), 1.30 (m, 32H), 0.97 (t, 3H, *J* = 7.0 Hz), 0.964 (t, 3H, *J* = 7.1 Hz), 0.957 (t, 3H, *J* = 7.1 Hz), 0.94 (t, 3H, *J* = 7.2 Hz), 0.90 (t, 6H, *J* = 6.8 Hz), 0.89 (t, 3H, *J* = 6.9 Hz), 0.85 (t, 3H, *J* = 6.8 Hz) ppm. ^{13}C{^{1}H} NMR ($CDCl_3$, 150 MHz): δ 164.9, 152.4, 152.1, 151.8, 151.7, 151.0, 149.5, 149.36, 149.33, 149.28, 143.7, 143.4, 142.9, 142.1, 141.74, 141.65, 140.4, 139.7, 133.3, 130.4, 129.7, 128.9, 128.3, 127.3, 126.62, 126.56, 126.4, 124.5, 123.7, 123.4, 123.3, 123.2, 120.1, 108.8, 108.52, 108.46, 106.2, 106.04, 105.99, 69.62, 69.58, 69.56, 69.55, 69.13, 69.12, 69.11, 69.09, 32.12, 32.11, 32.08, 31.90, 31.88, 31.87, 29.91, 29.90, 29.88, 29.85, 29.833, 29.827, 29.81, 29.78, 29.74, 29.61, 29.59, 29.58, 29.55, 29.52, 29.51, 29.46, 29.44, 26.40, 26.39, 26.37, 26.05, 26.02, 26.01, 22.88, 22.87, 22.86, 22.840, 22.838, 22.836, 14.31, 14.30, 14.27, 14.244, 14.240, 14.237 ppm (17 carbon signals missing or overlapping). HRMS (ESI$^+$ of M + H$^+$): m/z for $C_{105}H_{150}N_4O_{10}$: calculated: 1628.1430; experimental: 1628.1425.

2,3,6,7-Tetrakis(hexyloxy)dibenzo[a,c]phenazine-11-yl 2,3,6,7-tetrakis(decyloxy)dibenzo[a,c]phenazine-11-carboxylate (dDBP(10,6)). A flame dried, three-neck round bottom flask (50 mL) equipped with a magnetic stir bar under nitrogen atmosphere was charged with dry CH_2Cl_2 (20 mL). The solvent was purged with nitrogen and **DBP-OH(6)** (36.8 mg, 0.0528 mmol), **DBP-A(10)** (51.0 mg, 0.0537 mmol), and DMAP (23.3 mg, 0.191 mmol) were added, in sequence. The dark yellow-brown suspension was stirred at 0 °C for 20 min. At this time, EDC (41.2 mg, 0.215 mmol) was added, and the yellow-brown mixture was gently refluxed for 1 hour to improve solubility, and then cooled and stirred at ambient temperature for 3 days. The resulting dark yellow-brown mixture was diluted with CH_2Cl_2 (25 mL) and subsequently washed with H_2O (3 * 25 mL), 10% v/v HCl (25 mL), and brine (25 mL), dried over $MgSO_4$ and concentrated on a rotary evaporator to afford a yellow-brown solid. The crude product was purified by column chromatography using a gradient of 90−100% CH_2Cl_2 in hexanes as the eluent (L = 13.7 cm, R_f = 0.20−0.29). The compound was further purified *via* recrystallization from ethyl acetate, yielding an orange powder (48.0 mg, 56%). ^{1}H NMR ($CDCl_3$, 400 MHz): δ 9.19 (d, 1H, *J* = 1.7 Hz), 8.640 (s, 1H), 8.637 (s, 1H), 8.62 (s, 1H), 8.59 (s, 1H), 8.52 (dd, 1H, *J* = 8.8, 1.8 Hz), 8.33 (d, 1H, *J* = 8.9 Hz), 8.32 (d, 1H, *J* = 9.1 Hz), 8.24 (d, 1H, *J* = 2.6 Hz), 7.77 (dd, 1H, *J* = 9.1, 2.5 Hz), 7.594 (s, 1H), 7.591 (s, 1H), 7.587 (s, 1H), 7.57 (s, 1H), 4.34 (t, 2H, *J* = 6.4 Hz), 4.322 (t, 2H, *J* = 6.5 Hz), 4.321 (m, 2H), 4.318 (t, 2H, *J* = 6.6 Hz), 4.27 (t, 2H, *J* = 7.0 Hz), 4.26 (t, 2H, *J* = 6.4 Hz), 4.25 (t, 2H, *J* = 6.6 Hz), 4.24 (t, 2H, *J* = 6.6 Hz), 1.99 (m, 16H), 1.62 (m, 16H), 1.43 (m, 32H), 1.31 (m, 32H), 0.97 (t, 3H, *J* = 6.9 Hz), 0.962 (t, 3H, *J* = 6.9 Hz), 0.958 (t, 3H, *J* = 6.9 Hz), 0.94 (t, 3H, *J* = 7.3 Hz), 0.90 (t, 3H, *J* = 6.7 Hz), 0.89 (t, 3H, *J* = 6.9 Hz), 0.88 (t, 3H, *J* = 7.3 Hz), 0.84 (t, 3H, *J* = 7.0 Hz) ppm. ^{13}C{^{1}H} NMR ($CDCl_3$, 150 MHz): δ 164.9, 152.4, 152.1, 151.8, 151.6, 151.0, 149.5, 149.34, 149.32, 149.27, 143.7, 143.4, 142.8, 142.1, 141.7, 141.6, 140.4, 139.7, 133.3, 130.4, 129.7, 128.9, 128.2, 127.3, 126.6, 126.5, 126.4, 124.5, 123.7, 123.4, 123.3, 123.2, 120.1, 108.8, 108.52, 108.50, 108.4, 106.1, 106.04, 105.99, 105.95, 69.59, 69.58, 69.56, 69.53, 69.13, 69.12, 69.09, 69.08, 32.13, 32.12, 32.11, 32.07, 31.91, 31.901, 31.896, 31.88, 29.93, 29.91, 29.88, 29.85, 29.83, 29.81, 29.78, 29.76, 29.60, 29.59, 29.58, 29.55, 29.54, 29.51, 29.49, 29.47, 26.42, 26.41, 26.39, 26.38, 26.06, 26.05, 26.04, 26.01, 22.89, 22.881, 22.878, 22.87, 22.853, 22.848, 22.83, 14.31, 14.303, 14.296, 14.27, 14.26, 14.250, 14.245 ppm (10 carbon signals missing or overlapping). Could not identify the M^+ peak in HRMS *via* ESI. MALDI-TOF ((M+1) + H^+ in DHBA): m/z for $C_{105}H_{150}N_4O_{10}$: calculated: 1629.146; experimental: 1629.076.

2,3,6,7-Tetrakis(decyloxy)dibenzo[a,c]phenazine-11-yl 2,3,6,7-tetrakis(decyloxy)dibenzo[a,c]phenazine-11-carboxylate (dDBP(10,10)). A flame dried, three-neck round bottom flask (50 mL) equipped with a magnetic stir bar under a nitrogen atmosphere was charged with dry CH_2Cl_2 (20 mL). The solvent was purged with nitrogen and **DBP-OH(10)** (69.1 mg, 0.0750 mmol), **DBP-A(10)** (73.3 mg, 0.0772 mmol), and DMAP (33.0 mg, 0.270 mmol) were added, in sequence. The dark yellow suspension was stirred at 0 °C for 20 min. At this time, EDC (69.5 mg, 0.363 mmol) was added, and the dark yellow mixture was gently refluxed for 1 hour to improve solubility, and then cooled and stirred at ambient temperature for 3 days. The resulting dark yellow-brown mixture was diluted with CH_2Cl_2 (25 mL) was subsequently washed with H_2O (3 * 25 mL), 10% v/v HCl (25 mL), and brine (25 mL), dried over $MgSO_4$ and concentrated on a rotary evaporator to afford a yellow-brown solid. The crude product was purified by column chromatography using a gradient of 70−100% CH_2Cl_2 in hexanes as the eluent (L = 13.5 cm, R_f = 0.21−0.78). The compound was further purified *via* recrystallization from ethyl acetate, yielding an orange powder (57.9 mg, 42%). ^{1}H NMR ($CDCl_3$, 400 MHz): δ 9.18 (d, 1H, *J* = 1.8 Hz), 8.628 (s, 1H), 8.627 (s, 1H), 8.61 (s, 1H), 8.57 (s, 1H), 8.52 (dd, 1H, *J* = 8.8, 2.0 Hz), 8.33 (d, 1H, *J* = 8.8 Hz), 8.31 (d, 1H, *J* = 9.2 Hz), 8.23 (d, 1H, *J* = 2.6 Hz), 7.76 (dd, 1H, *J* = 9.1, 2.6 Hz), 7.59 (s, 1H), 7.580 (s, 1H), 7.579 (s, 1H), 7.56 (s, 1H), 4.34 (t, 2H, *J* = 7.0 Hz), 4.32 (t, 2H, *J* = 6.6 Hz), 4.31 (t, 2H, *J* = 6.6 Hz), 4.30 (t, 2H, *J* = 6.8 Hz), 4.27 (t, 2H, *J* = 6.7 Hz), 4.25 (t, 2H, *J* = 6.8 Hz), 4.24 (t, 2H, *J* = 6.8 Hz), 4.23 (t, 2H, *J* = 6.5 Hz), 1.99 (m, 16H), 1.61 (m, 16H), 1.45 (m, 16H), 1.31 (m, 80H), 0.90 (t, 3H, J = 6.8 Hz), 0.894 (m, 9H), 0.891 (t, 3H, *J* = 6.8 Hz), 0.88 (t, 3H, *J* = 6.6 Hz), 0.85 (t, 3H, *J* = 6.9 Hz), 0.84 (t, 3H, *J* = 6.9 Hz) ppm. ^{13}C{^{1}H} NMR ($CDCl_3$, 150 MHz): δ 164.9, 152.4, 152.1, 151.8, 151.7, 151.0, 149.53, 149.52, 149.39, 149.37, 149.32, 143.7, 143.5, 142.9, 142.2, 141.8, 141.7, 140.5, 139.8, 133.3, 130.4, 129.8, 127.3, 126.7, 126.6, 126.4, 124.6, 123.7, 123.5, 123.3, 120.1, 108.9, 108.6, 108.5, 106.2, 106.07, 106.05, 69.643, 69.637, 69.62, 69.59, 69.16, 69.15, 69.13, 69.11, 32.12, 32.11, 32.08, 32.07, 29.92, 29.90, 29.88, 29.87, 29.84, 29.83, 29.80, 29.77, 29.74, 29.59, 29.58, 29.555, 29.547, 29.52, 26.40, 26.39, 26.38, 26.37, 22.884, 22.876, 22.841, 22.836, 14.31, 14.30, 14.27, 14.26 ppm (45 carbon signals missing or overlapping). HRMS (ESI$^+$ of M + H$^+$): m/z for $C_{121}H_{182}N_4O_{10}$: calculated: 1852.3934; experimental: 1852.3918.

2,3,6,7-Tetrakis(hexyloxy)dibenzo[a,c]phenazine-11-yl 2,3,6,7,12-pentakis(hexyloxy)dibenzo[a,c]phenazine-11-carboxylate (dDBP-OHx(6,6)). A flame dried, three-neck round bottom flask (50 mL) equipped with a magnetic stir bar under a nitrogen atmosphere was charged with dry CH_2Cl_2 (20 mL). The solvent was purged with nitrogen and **DBP-A(6,OHx)** (54.9 mg, 0.0665 mmol), **DBP-OH(6)** (70.3 mg, 0.101 mmol), and DMAP (26.2 mg, 0.214 mmol) were added, in sequence. The dark orange suspension was stirred at 0 °C for 20 min. At this time, EDC (54.0 mg, 0.282 mmol) was added, and the yellow-brown mixture was stirred at ambient temperature for 22 hours. The resulting dark orange-brown mixture was diluted with CH_2Cl_2 (25 mL) and subsequently washed with H_2O (3 * 25 mL), 10% v/v HCl (25 mL), and brine (25 mL), dried over $MgSO_4$ and concentrated on a rotary evaporator to afford a yellow-orange solid. The crude product was purified by column chromatography using a gradient of 80−100% CH_2Cl_2 in hexanes as the eluent (L = 15.6 cm, R_f = 0.22−0.26). The compound was further purified *via* recrystallization from EtOH in CH_2Cl_2, yielding an orange powder (37.9 mg, 38%). ^{1}H NMR ($CDCl_3$, 400 MHz): δ 8.97 (s, 1H), 8.74 (s, 1H), 8.73 (s, 1H), 8.71 (s, 1H), 8.67 (s, 1H), 8.36 (d, 1H, *J* = 9.1 Hz), 8.28 (d, 1H, *J* = 2.6 Hz), 7.79 (dd, 1H, *J* = 9.1, 2.6 Hz), 7.68 (s, 2H), 7.67 (s, 3H), 4.35 (m, 10H), 4.28 (t, 4H, *J* = 6.2 Hz), 4.27 (t, 4H, *J* = 6.3 Hz), 1.99 (m, 18H), 1.62 (m, 18H), 1.42 (m, 36H), 0.964 (t, 3H, *J* = 7.1 Hz), 0.955 (t, 6H, *J* = 7.0 Hz), 0.953 (t, 6H, *J* = 6.8 Hz), 0.949 (t, 6H, *J* = 7.5 Hz), 0.94 (t, 3H, *J* = 7.0 Hz), 0.89 (t, 3H, *J* = 7.1 Hz) ppm. ^{13}C{^{1}H} NMR ($CDCl_3$, 150 MHz): δ 164.0, 157.9, 152.3, 151.9, 151.8, 151.6, 151.1, 149.6, 149.44, 149.40, 149.35, 144.5, 143.4, 142.2, 141.9, 141.7, 141.1, 139.8, 136.3, 134.3, 130.4, 127.4, 126.7, 126.5, 126.0, 124.7, 124.2, 123.82, 123.80, 123.6, 123.4, 120.0, 108.8, 108.7, 108.6, 108.2, 108.1, 106.4, 106.3, 106.09, 106.08, 69.72, 69.67, 69.66, 69.65, 69.57, 69.56, 69.54, 69.19, 69.16, 69.14, 31.87, 31.86, 31.85, 31.73, 29.500, 29.498, 29.48, 29.47, 29.45, 29.43, 29.42, 29.28, 26.04, 26.03, 26.01, 25.992, 25.986, 22.85, 22.83, 22.82, 22.77, 14.26, 14.24, 14.23, 14.21 ppm (19 carbon signals missing or overlapping). HRMS (ESI$^+$ of M + H$^+$): m/z for $C_{95}H_{130}N_4O_{11}$: calculated: 1503.9814; experimental: 1503.9823.

2,3,6,7-Tetrakis(decyloxy)dibenzo[a,c]phenazine-11-yl 2,3,6,7,12-pentakis(hexyloxy)dibenzo[a,c]phenazine-11-carboxylate (dDBP-OHx(6,10)). A flame dried, three-neck round bottom flask (50 mL) equipped with a magnetic stir bar under a nitrogen atmosphere was charged with dry CH_2Cl_2 (20 mL). The solvent was purged with nitrogen and **DBP-OH(10)** (62.9 mg, 0.0683 mmol), **DBP-A(6,OHx)** (57.1 mg, 0.0692 mmol), and DMAP (29.5 mg, 0.241 mmol) were added, in sequence. The orange-brown suspension was stirred at 0 °C for 20 min. At this time, EDC (80.9 mg, 0.422 mmol) was added, and the yellow-brown mixture was gently refluxed for 2 hours to improve solubility, and then cooled and stirred at ambient temperature for 3 days. The resulting dark yellow-brown mixture was diluted with CH_2Cl_2 (25 mL) and subsequently washed with H_2O (3 * 25 mL, 10% v/v HCl (25 mL), and brine (25 mL), dried over $MgSO_4$ and concentrated on a rotary evaporator to afford a yellow-brown solid. The crude product was purified by column chromatography using a gradient of 90−100% CH_2Cl_2 in hexanes as the eluent (L = 13.2 cm, R_f = 0.22−0.23). The compound was further purified *via* recrystallization from ethyl acetate, yielding an orange powder (69.2 mg, 59%). ^{1}H NMR ($CDCl_3$, 400 MHz): δ 8.93 (s, 1H), 8.68 (s, 1H), 8.660 (s, 1H), 8.658 (s, 1H), 8.61 (s, 1H), 8.34 (d, 1H, *J* = 9.1 Hz), 8.26 (d, 1H, *J* = 2.5 Hz), 7.78 (dd, 1H, *J* = 9.1, 2.5 Hz), 7.633 (s, 1H), 7.626 (s, 1H), 7.625 (s, 1H), 7.624 (s, 1H), 7.61 (s, 1H), 4.35 (t, 2H, *J* = 6.4 Hz), 4.338 (m, 4H), 4.336 (t, 2H, *J* = 6.4 Hz), 4.33 (t, 2H, *J* = 6.7 Hz), 4.27 (t, 2H, *J* = 6.7 Hz), 4.26 (m, 2H), 4.254 (t, 2H, *J* = 6.7 Hz), 4.249 (t, 2H, *J* = 6.5 Hz), 1.99 (m, 18H), 1.61 (m, 18H), 1.43 (m, 36H), 1.30 (m, 32H), 0.97 (t, 3H, *J* = 7.1 Hz), 0.964 (t, 3H, *J* = 7.2 Hz), 0.958 (t, 3H, *J* = 7.0 Hz), 0.93 (t, 3H, *J* = 7.2 Hz), 0.898 (t, 3H, *J* = 7.1 Hz), 0.895 (t, 3H, *J* = 6.9 Hz), 0.891 (t, 3H, *J* = 7.2 Hz), 0.887 (t, 3H, *J* = 7.1 Hz), 0.85 (t, 3H, *J* = 7.0 Hz) ppm. ^{13}C{^{1}H} NMR ($CDCl_3$, 150 MHz): δ 163.9, 157.9, 152.2, 151.8, 151.7, 151.5, 151.1, 149.5, 149.4, 149.34, 149.28, 144.5, 143.4, 142.1, 141.9, 141.7, 141.1, 139.8, 136.2, 134.4, 130.4, 127.3, 126.6, 126.4, 125.9, 124.7, 124.1, 123.7, 123.5, 123.3, 120.1, 108.7, 108.6, 108.5, 108.1, 108.0, 106.3, 106.2, 106.1, 106.0, 69.66, 69.63, 69.61, 69.54, 69.52, 69.15, 69.14, 69.12, 69.10, 32.12, 32.11, 32.08, 31.89, 31.88, 31.873, 31.867, 31.75, 29.91, 29.90, 29.88, 29.83, 29.82, 29.81, 29.76, 29.74, 29.59, 29.58, 29.55, 29.54, 29.53, 29.49, 29.45, 29.3, 26.39, 26.38, 26.37, 26.07, 26.05, 26.01, 26.00, 22.874, 22.868, 22.86, 22.84, 22.83, 22.77, 14.31, 14.30, 14.27, 14.23, 14.22 ppm (30 carbon signals missing or overlapping). Could not identify the M^+ peak in HRMS *via* ESI. MALDI-TOF ((M+1) + H^+ in DHBA): m/z for $C_{111}H_{162}N_4O_{11}$: calculated: 1729.235; experimental: 1729.249.

1.3. NMR Spectra

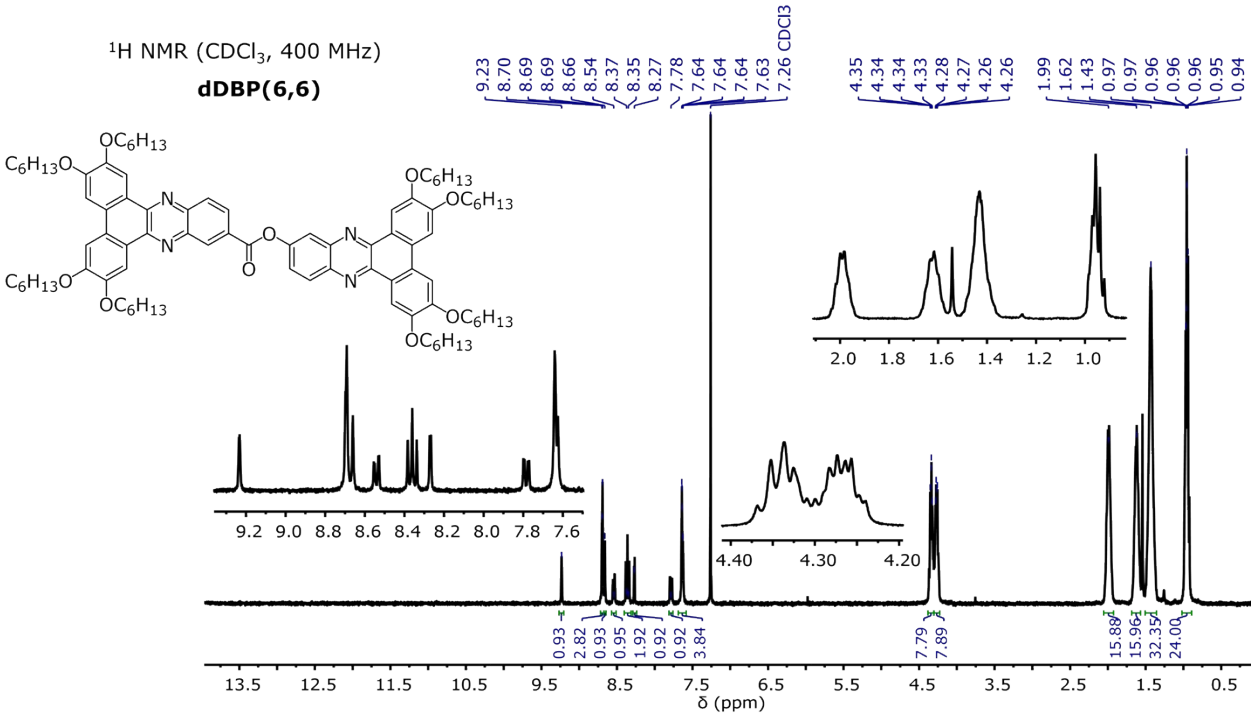

Figure S1. ^{1}H NMR spectrum of **dDBP(6,6)**.

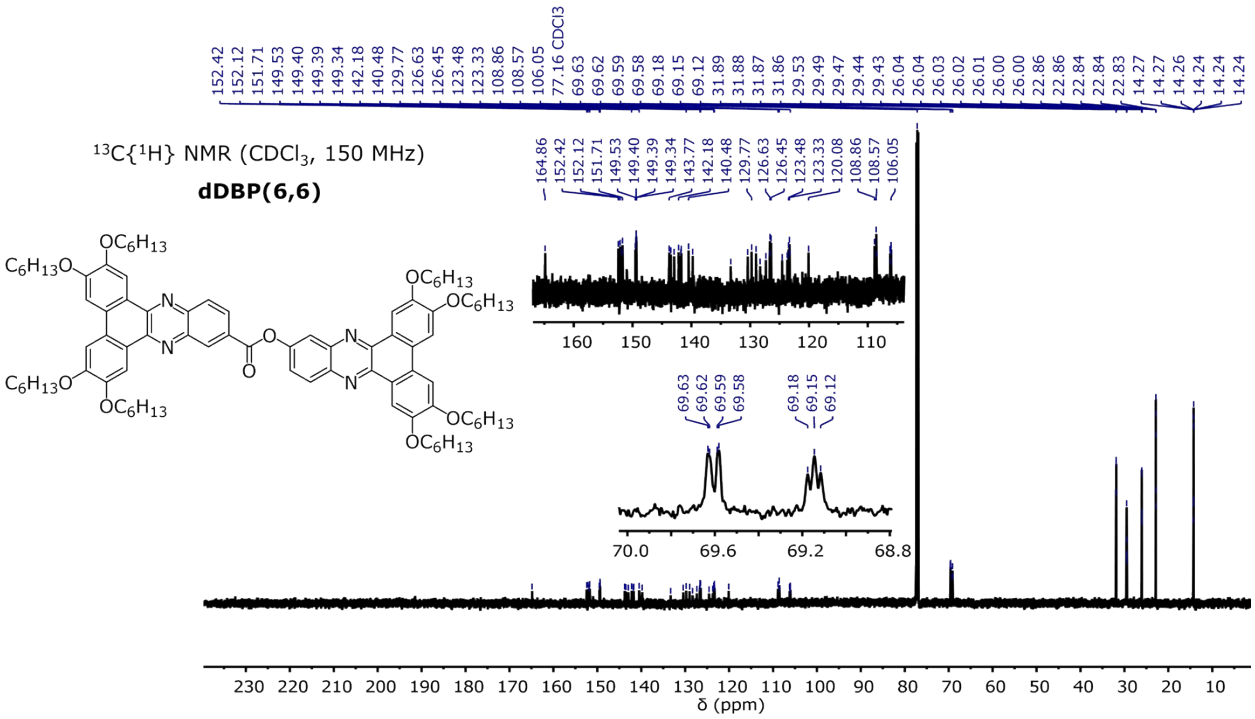

Figure S2. ^{13}C{^{1}H} NMR spectrum of **dDBP(6,6)**.

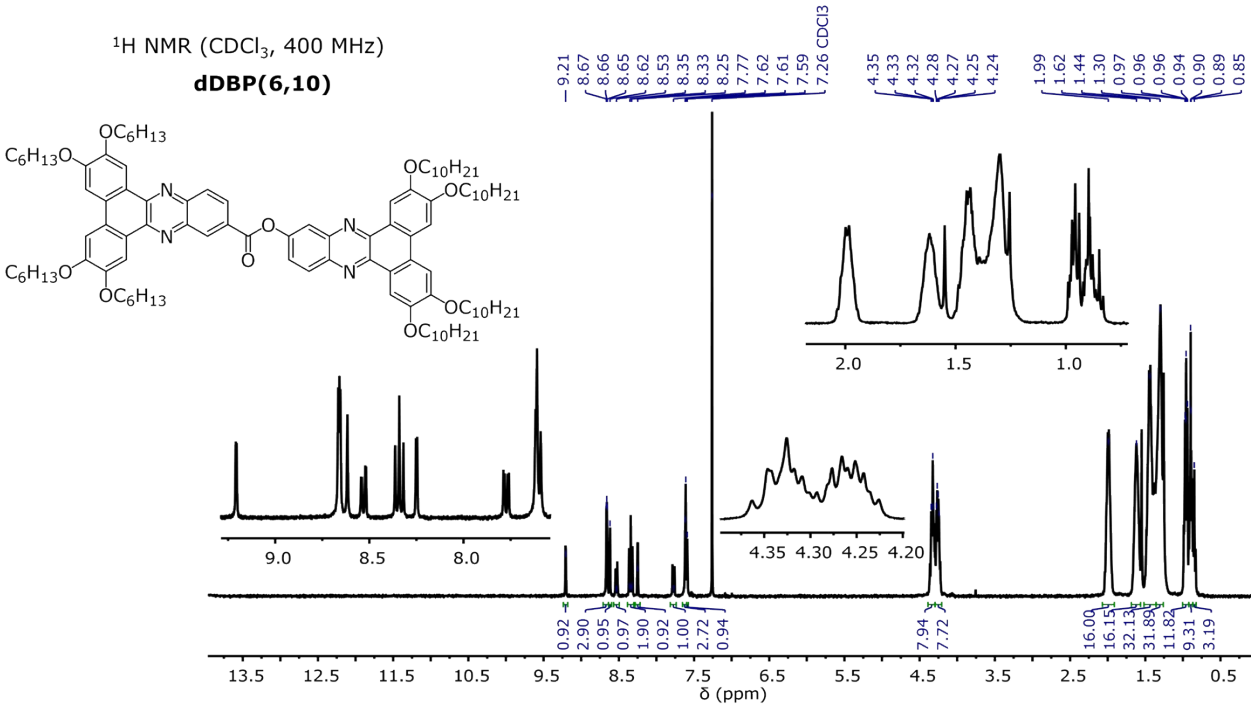

Figure S3. ^{1}H NMR spectrum of **dDBP(6,10)**.

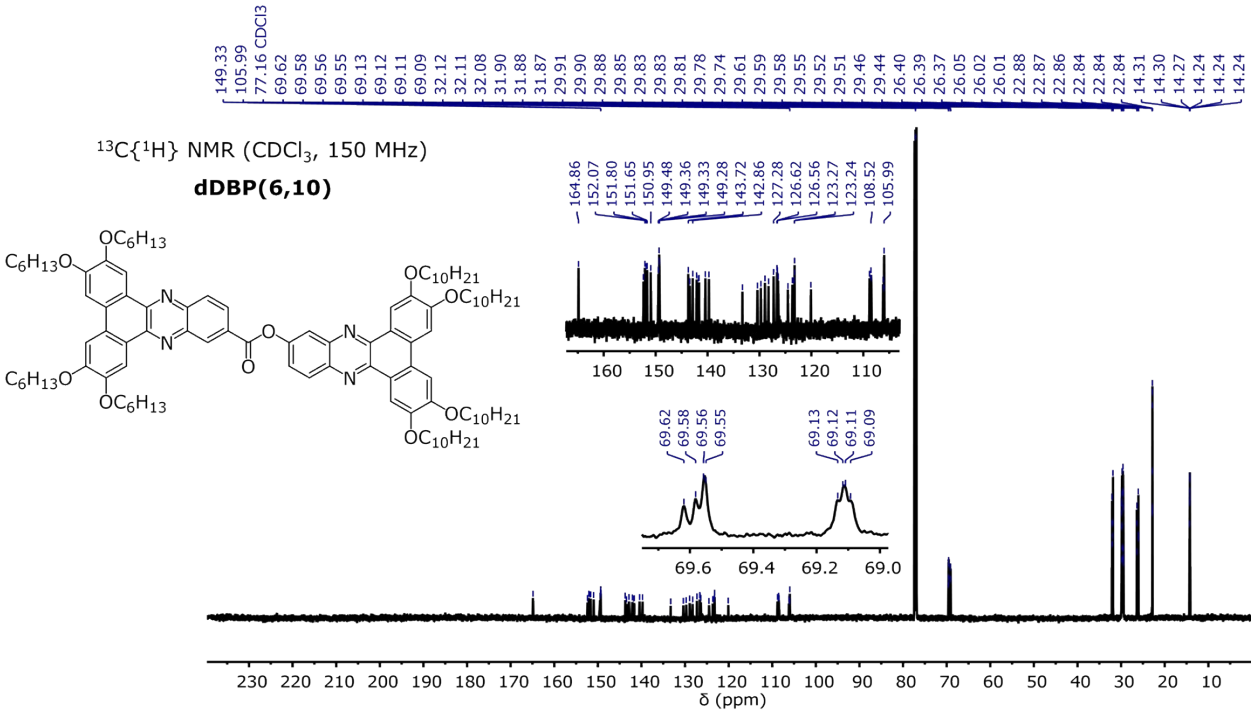

Figure S4. ^{13}C{^{1}H} NMR spectrum of **dDBP(6,10)**.

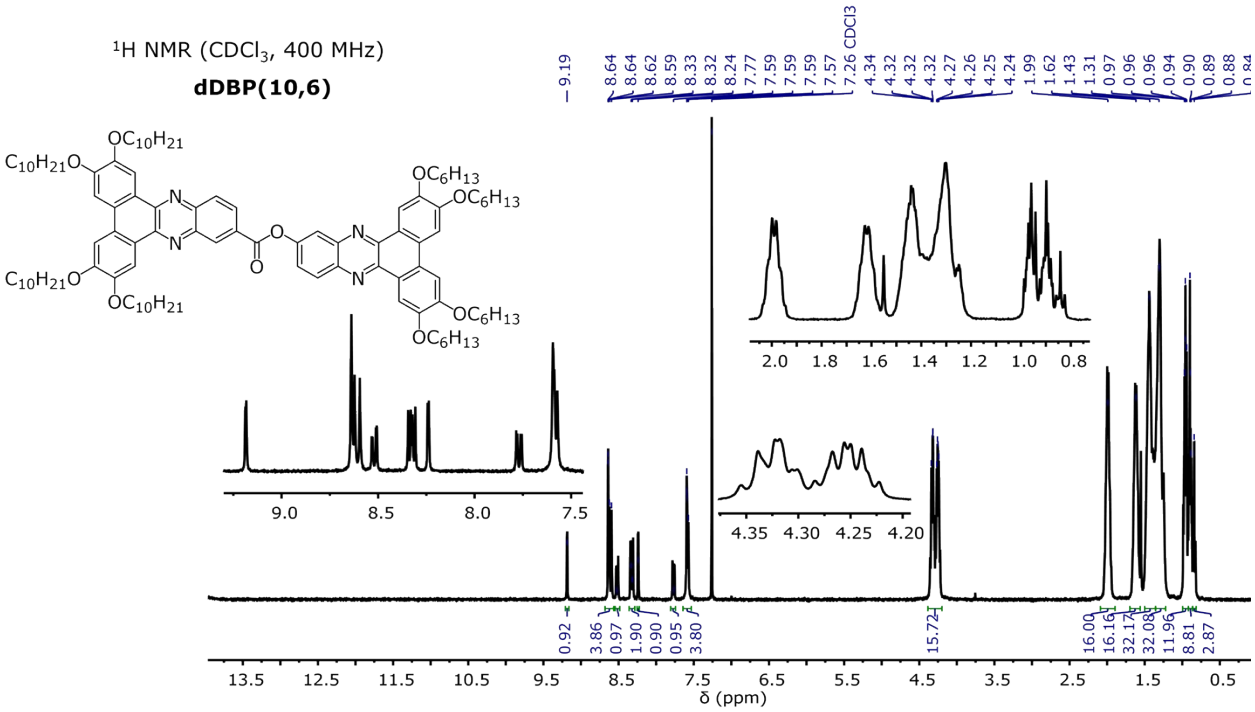

Figure S5. ^{1}H NMR spectrum of **dDBP(10,6)**.

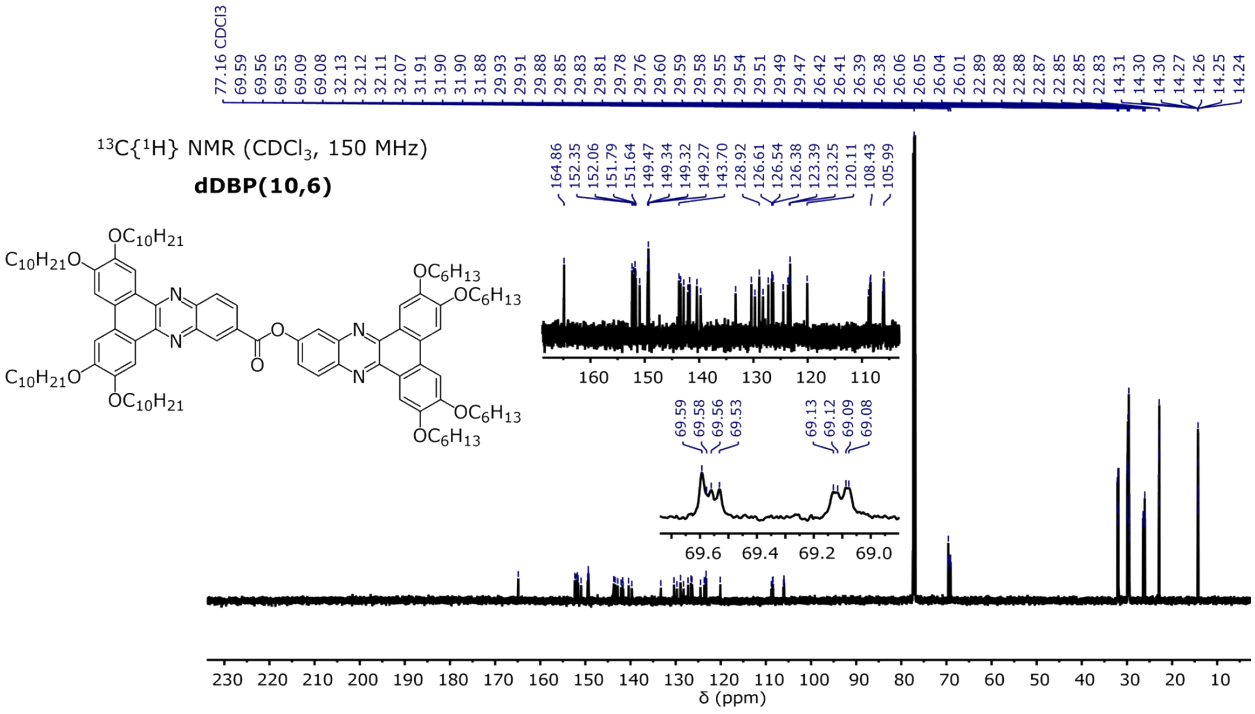

Figure S6. ^{13}C{^{1}H} NMR spectrum of **dDBP(10,6)**.

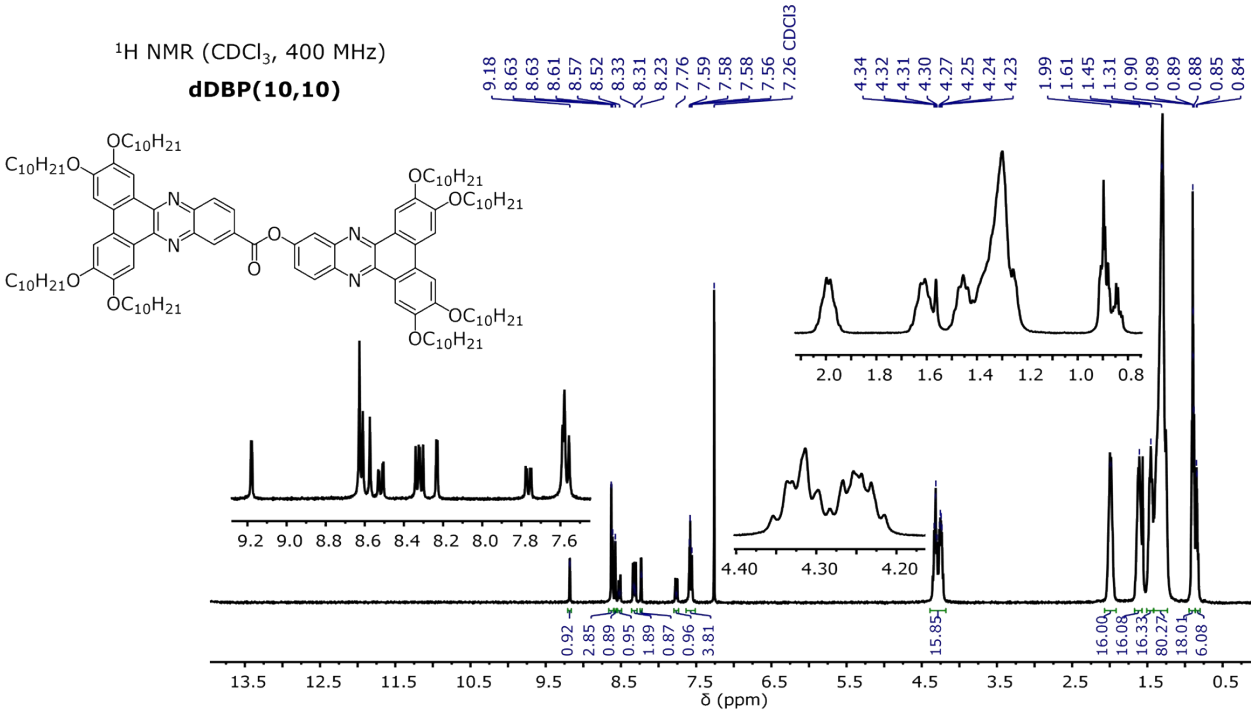

Figure S7. ^{1}H NMR spectrum of **dDBP(10,10)**.

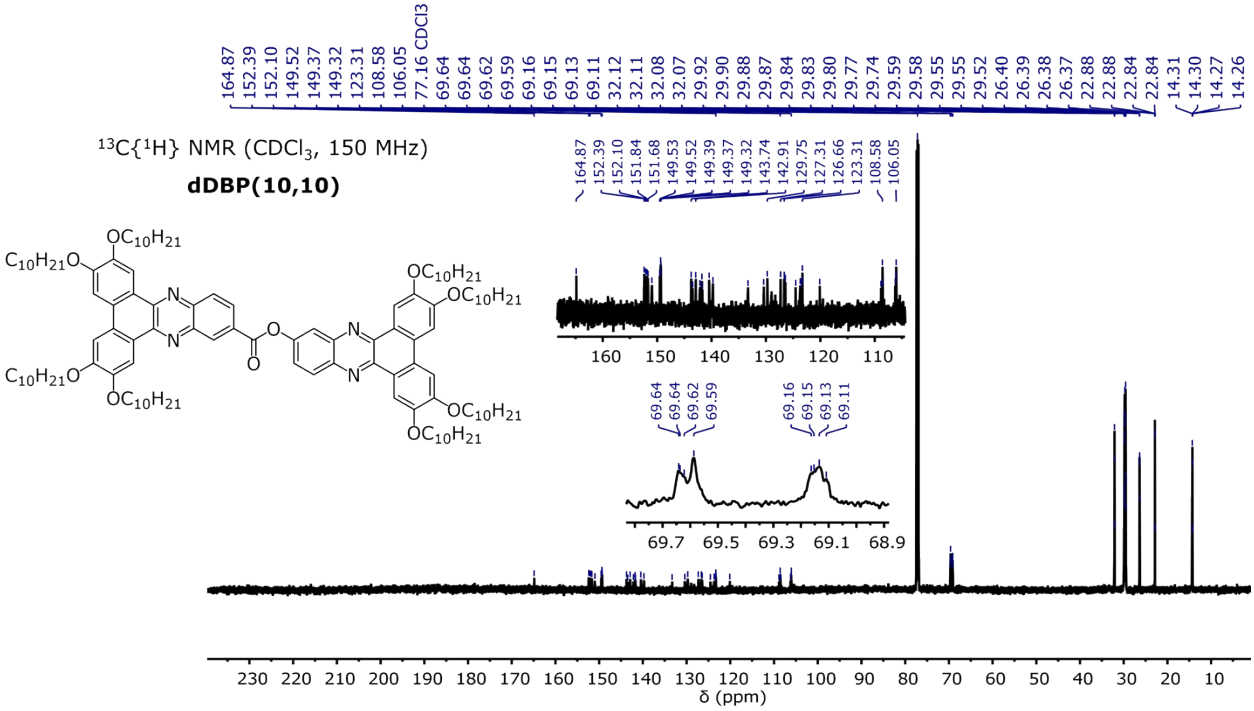

Figure S8. ^{13}C{^{1}H} NMR spectrum of **dDBP(10,10)**.

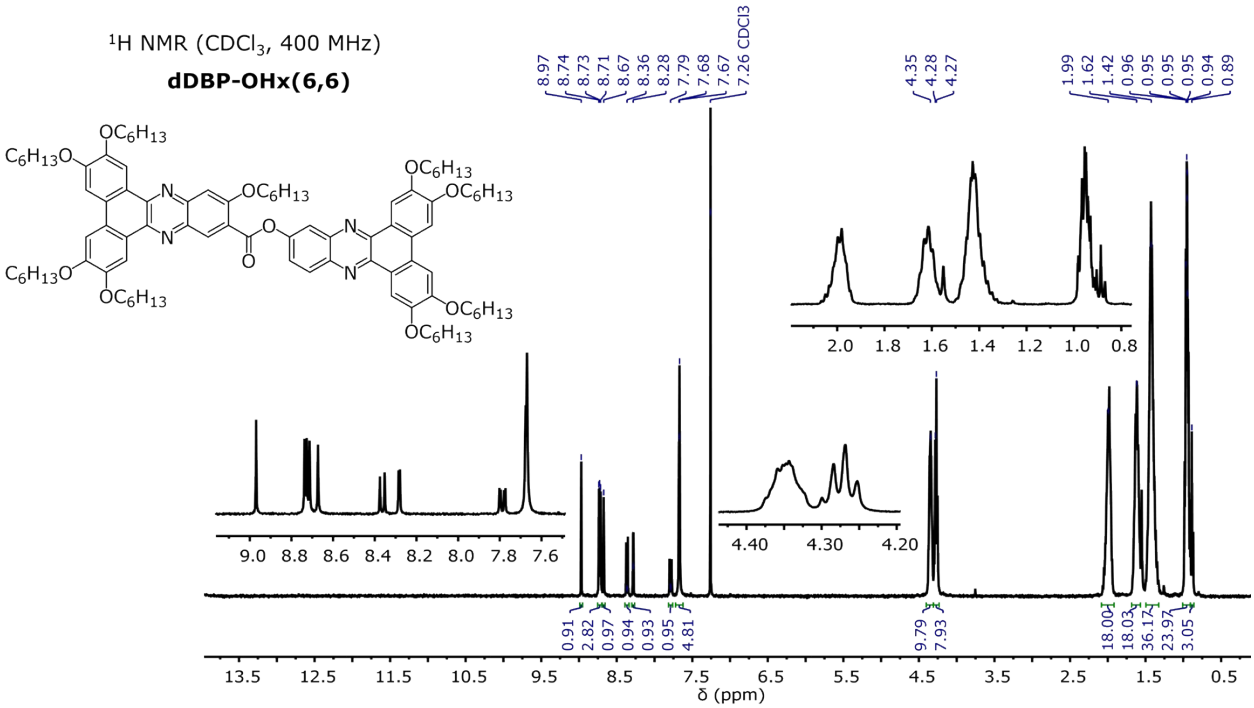

Figure S9. ^{1}H NMR spectrum of **dDBP-OHx(6,6)**.

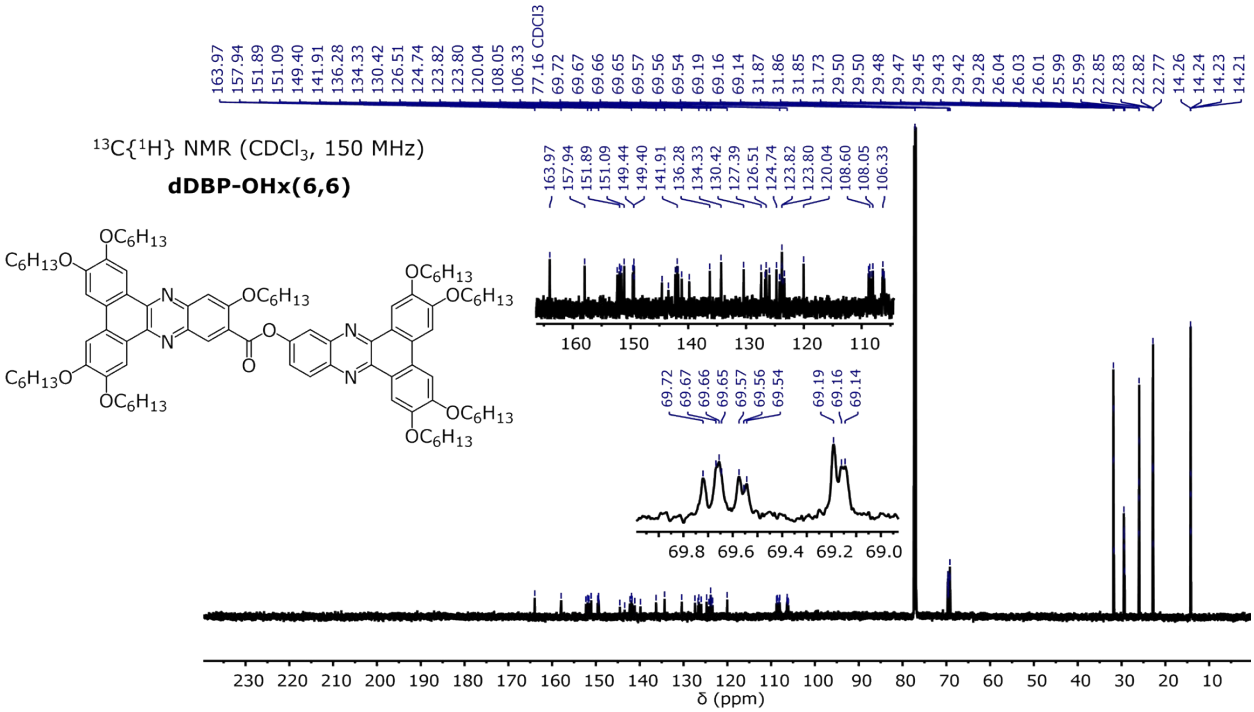

Figure S10. ^{13}C{^{1}H} NMR spectrum of **dDBP-OHx(6,6)**.

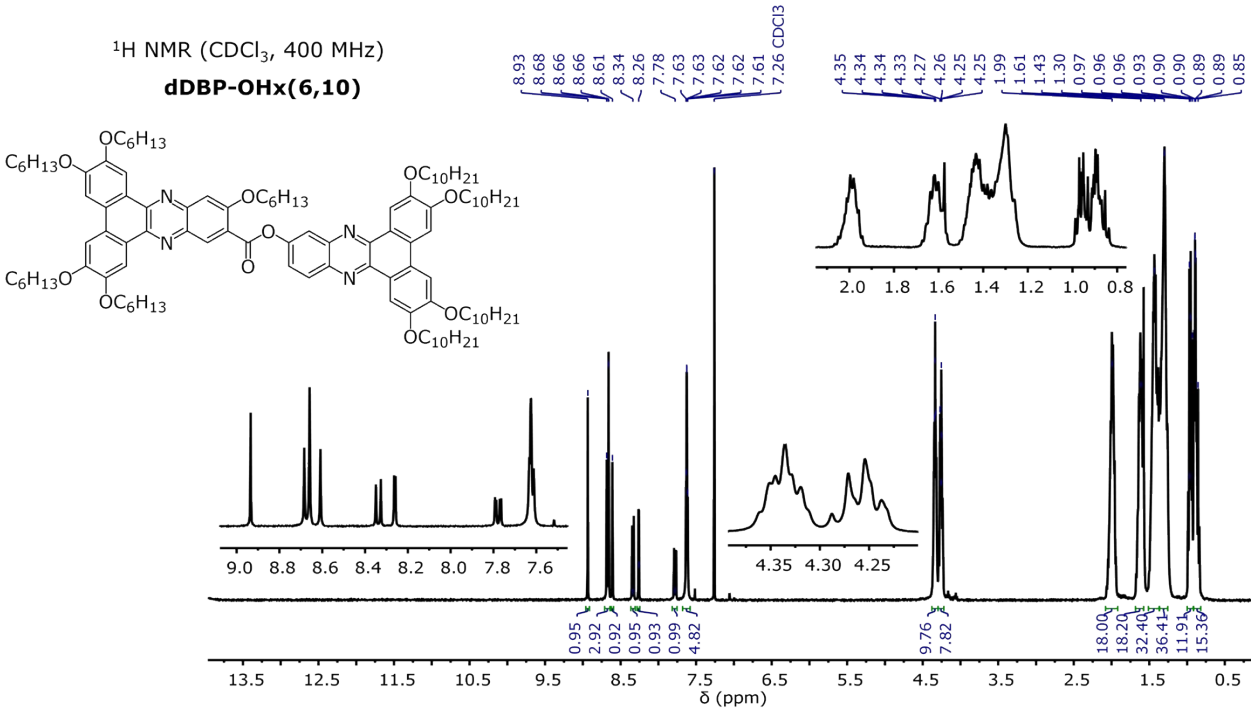

Figure S11. ^{1}H NMR spectrum of **dDBP-OHx(6,10)**.

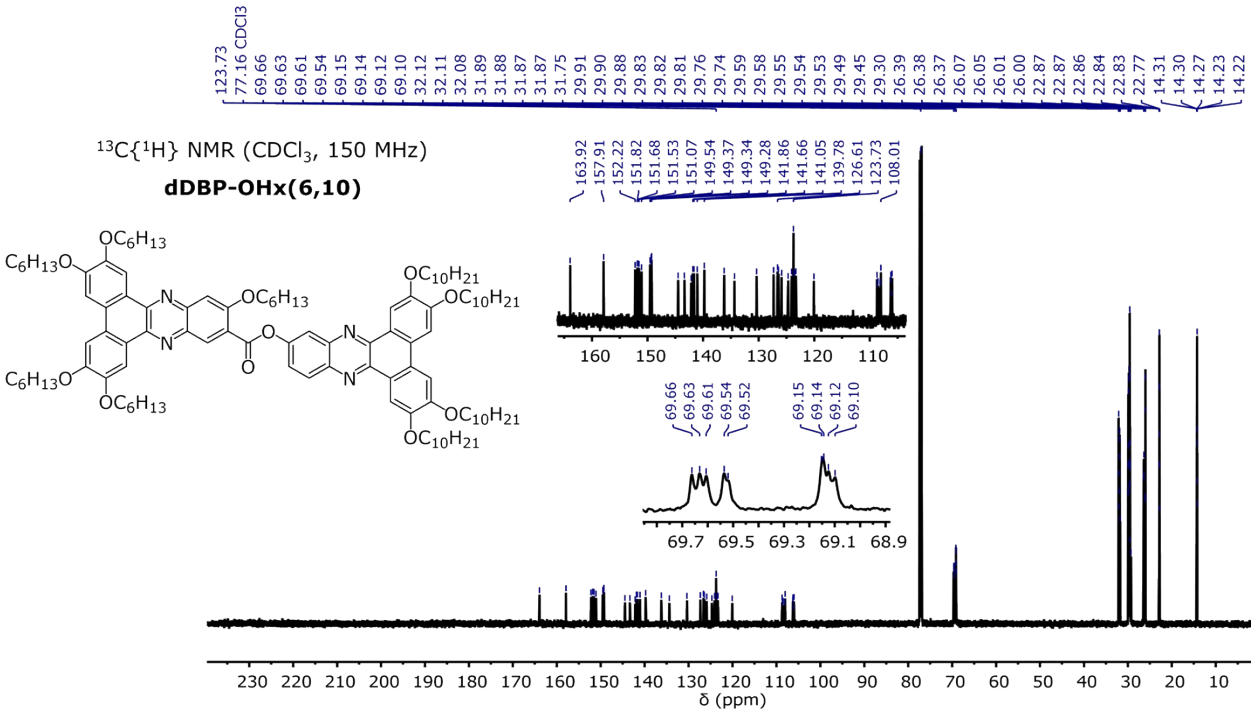

Figure S12. ^{13}C{^{1}H} NMR spectrum of **dDBP-OHx(6,10)**.

2. Differential Scanning Calorimetry (DSC)

Phase transition temperatures and enthalpies were investigated using differential scanning calorimetry (DSC) on a DSC Q2000 instrument (TA Instruments) equipped with a refrigerated cooling system (TA Instruments, Refrigerated Cooling System 90). Heating and cooling measurements were performed at a rate of 10 °C/min.

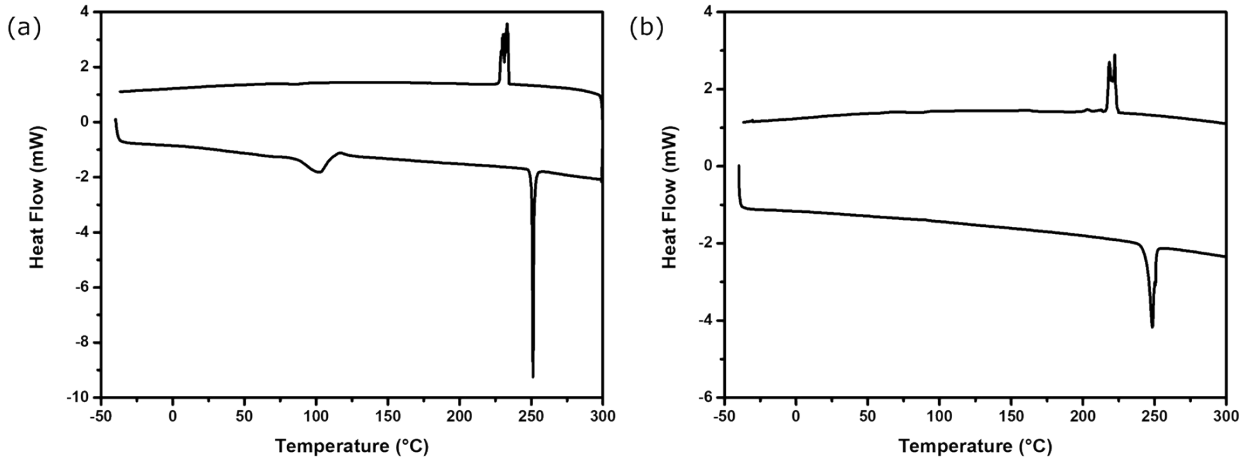

Figure S13. DSC thermograms of **dDBP(6,6)** for the (a) first and (b) second heating/cooling cycles.

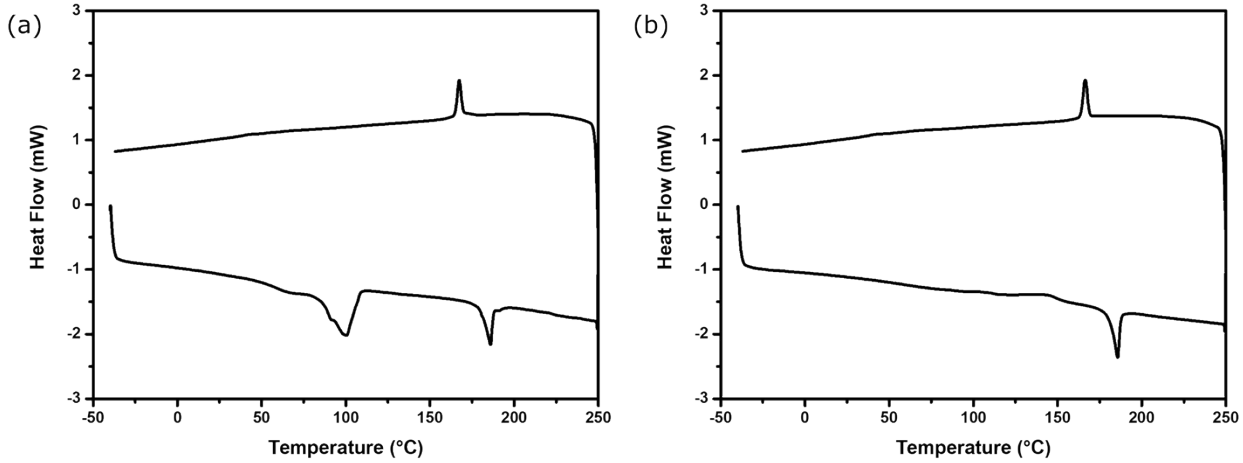

Figure S14. DSC thermograms of **dDBP(6,10)** for the (a) first and (b) second heating/cooling cycles.

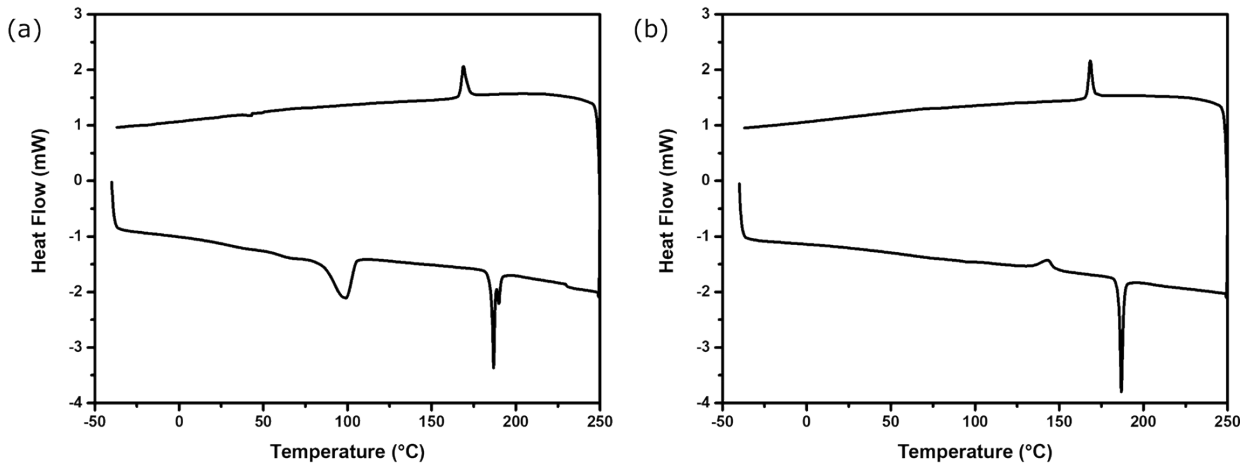

Figure S15. DSC thermograms of **dDBP(10,6)** for the (a) first and (b) second heating/cooling cycles.

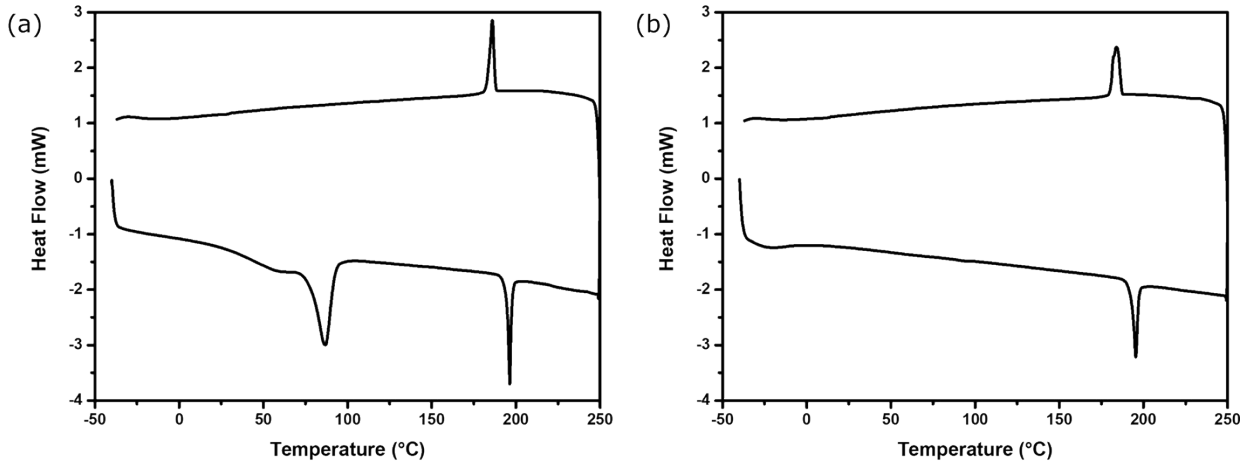

Figure S16. DSC thermograms of **dDBP(10,10)** for the (a) first and (b) second heating/cooling cycles.

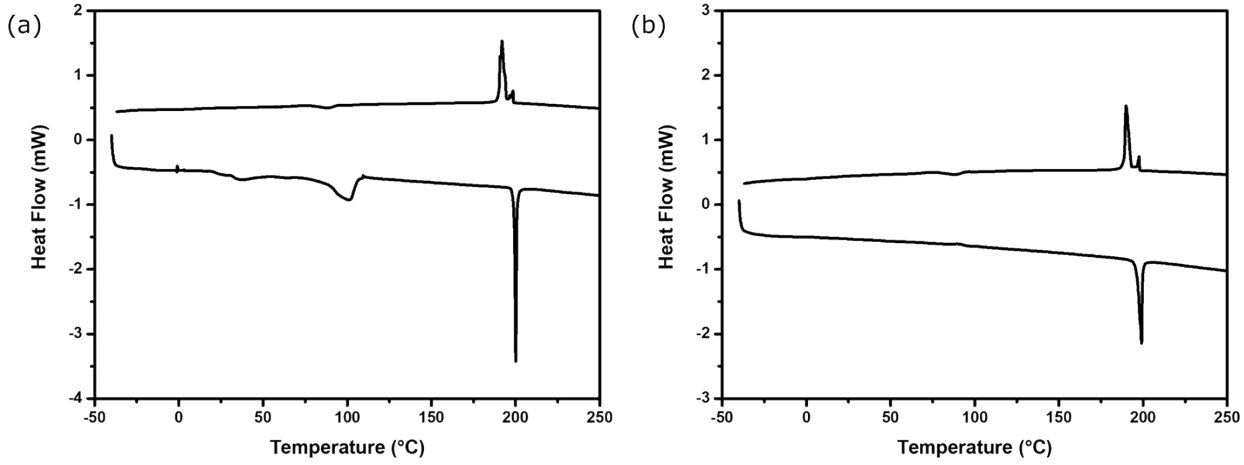

Figure S17. DSC thermograms of **dDBP-OHx(6,6)** for the (a) first and (b) second heating/cooling cycles.

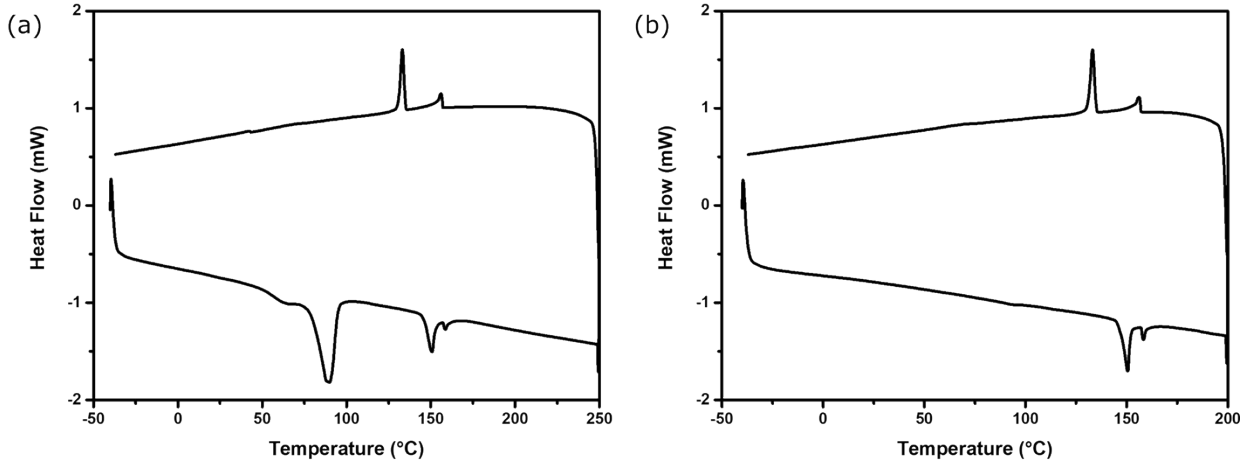

Figure S18. DSC thermograms of **dDBP-OHx(6,10)** for the (a) first and (b) second heating/cooling cycles.

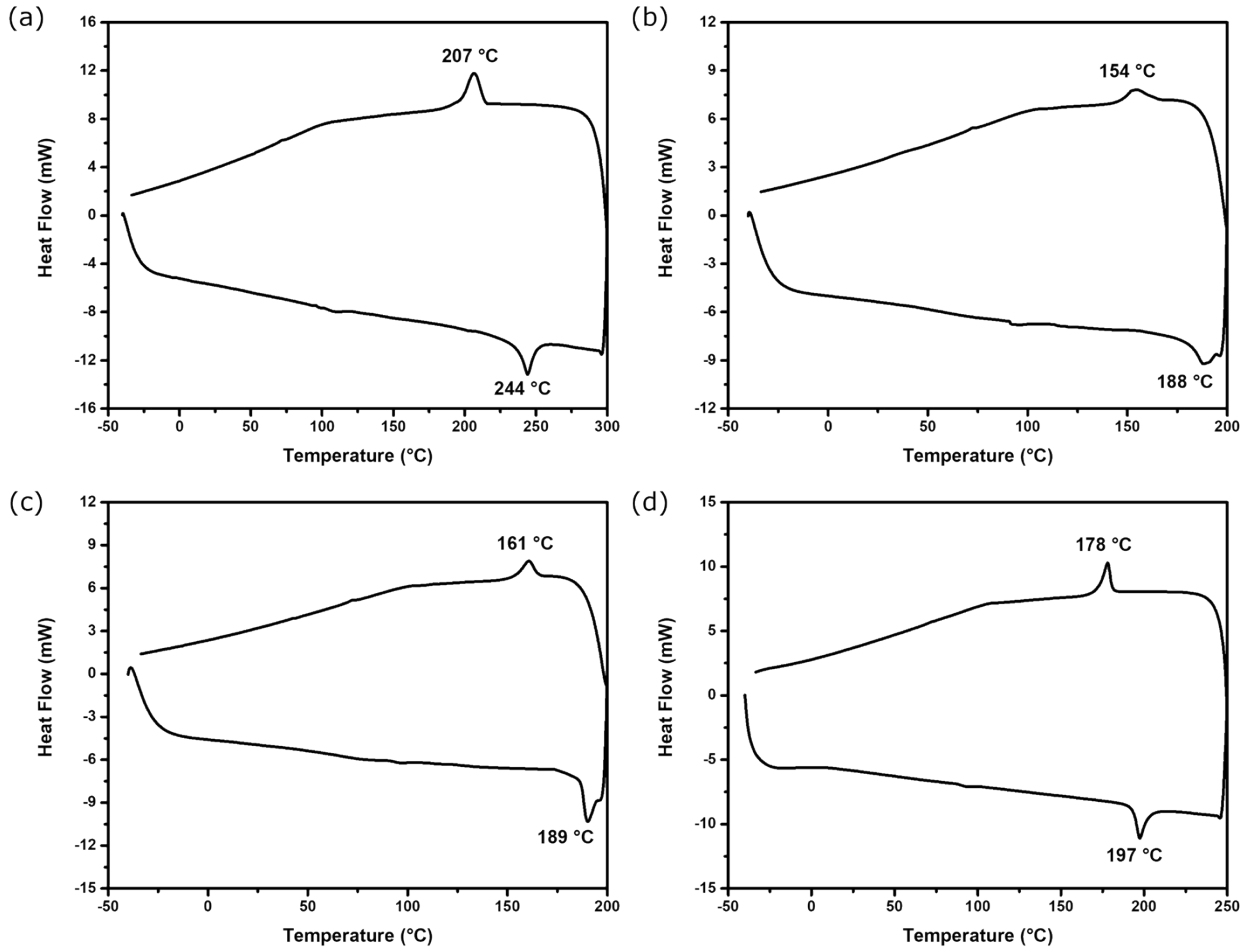

Figure S19. DSC thermograms of (a) **dDBP(6,6)**, (b) **dDBP(6,10)**, (c) **dDBP(10,6)**, and (d) **dDBP(10,10)** at a heating/cooling rate of 50 °C/min.

3. Polarized Optical Microscopy (POM)

Texture and phase behaviour analyses were carried out using polarized optical microscopy (POM) on an Olympus BX50 microscope equipped with cross polarizers and a Linkam LTS350 heating stage. All images shown are ca. 920 x 1400 μm in size, unless otherwise specified.

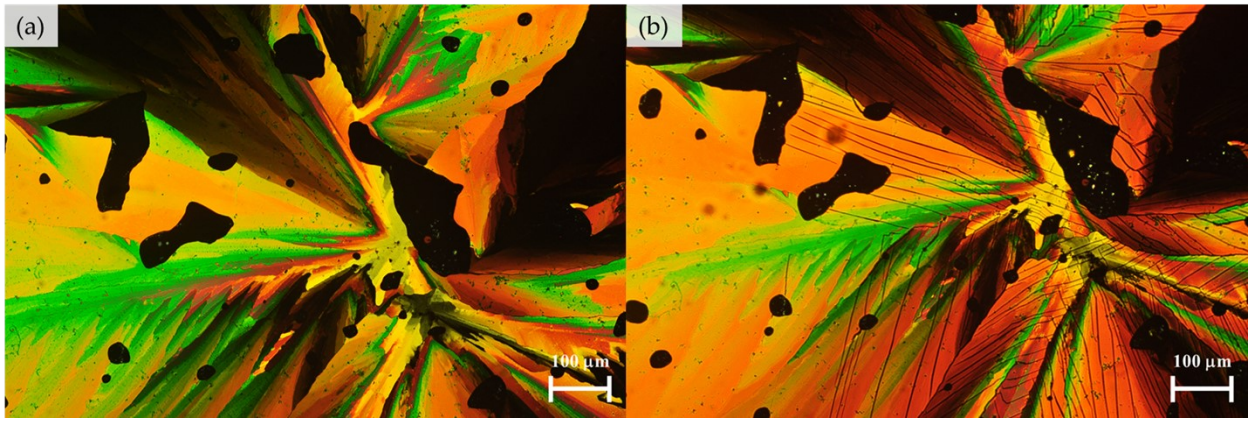

Figure S20. Polarized optical micrographs of **dDBP(6,6)** displaying birefringent textures of the crystalline phase at (a) 218 °C and (b) room temperature. Images were taken in the same plane of view.

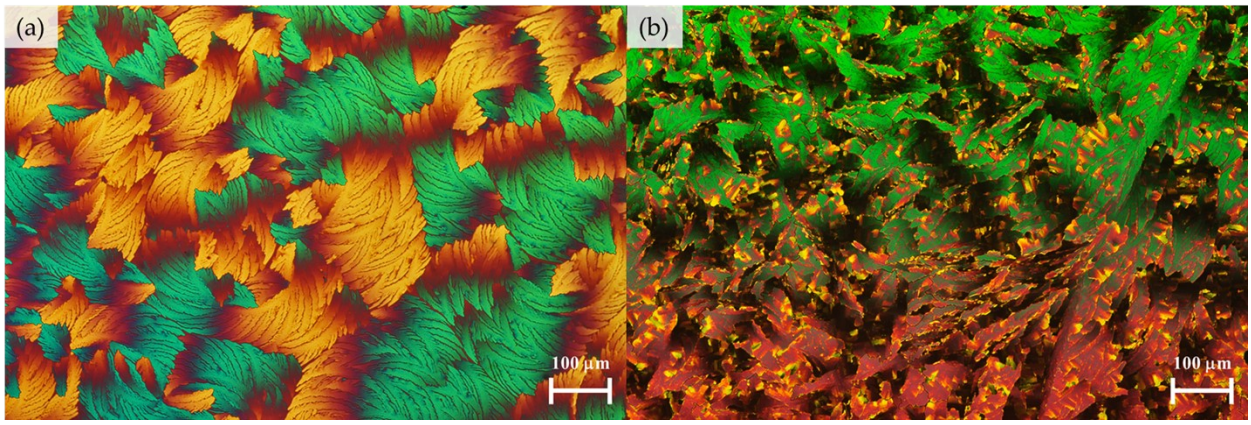

Figure S21. Polarized optical micrographs of **dDBP(6,10)** displaying birefringent textures of the crystalline phase at (a) 166 °C and (b) room temperature. Image (a) was taken with a 530 nm quarter wavelength retardation plate.

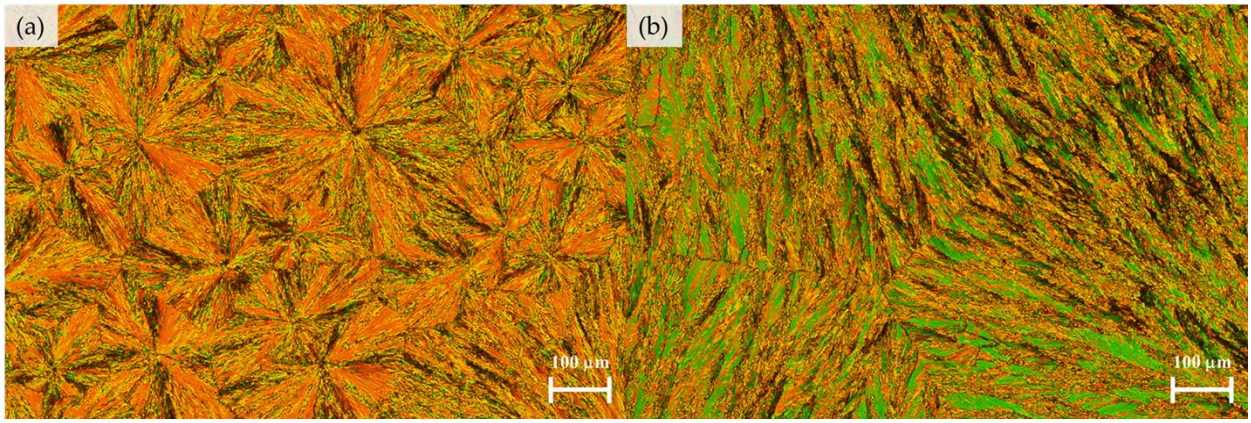

Figure S22. Polarized optical micrographs of **dDBP(10,6)** displaying spherulitic textures of the crystalline phase at (a) 161 °C and (b) room temperature.

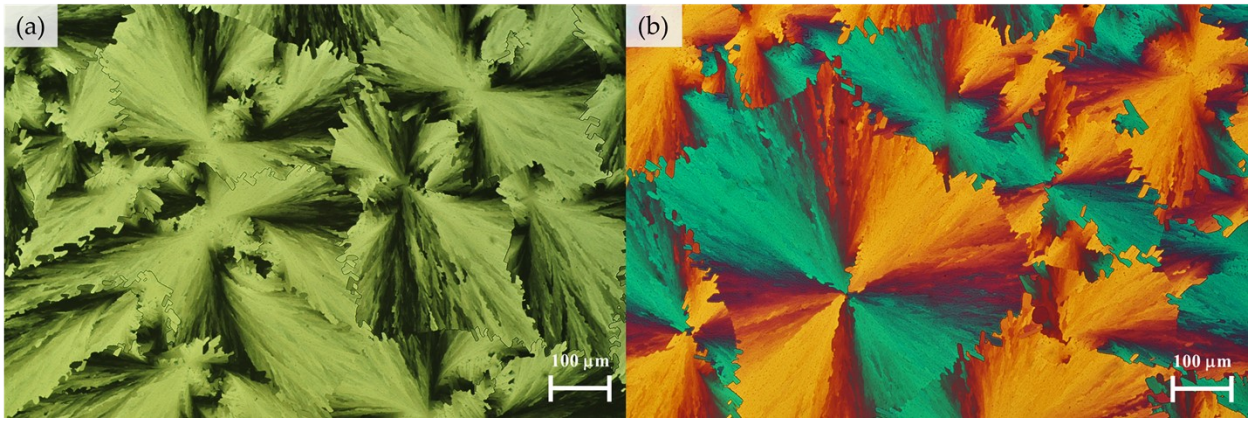

Figure S23. Polarized optical micrographs of **dDBP(10,10)** displaying the spherulitic textures of the crystalline phase at (a) 179 °C and (b) room temperature. Image (b) was taken with a 530 nm quarter wavelength retardation plate.

4. Variable Temperature X-ray Diffraction (vt-XRD)

Wide-angle X-ray scattering (WAXS) experiments were obtained on a SAXSLAB Ganesha 300XL Small Angle X-ray Scattering (SAXS) system. All samples were loaded into thin-walled quartz capillary tubes (Charles Supper Company) with a 1.5 mm outer diameter. All measurements were performed using on a Linkam T95-PE heating stage. Figure S24 shows the WAXS spectra of a blank sample and **dDBP(6,6)** in the isotropic liquid phase, for reference.

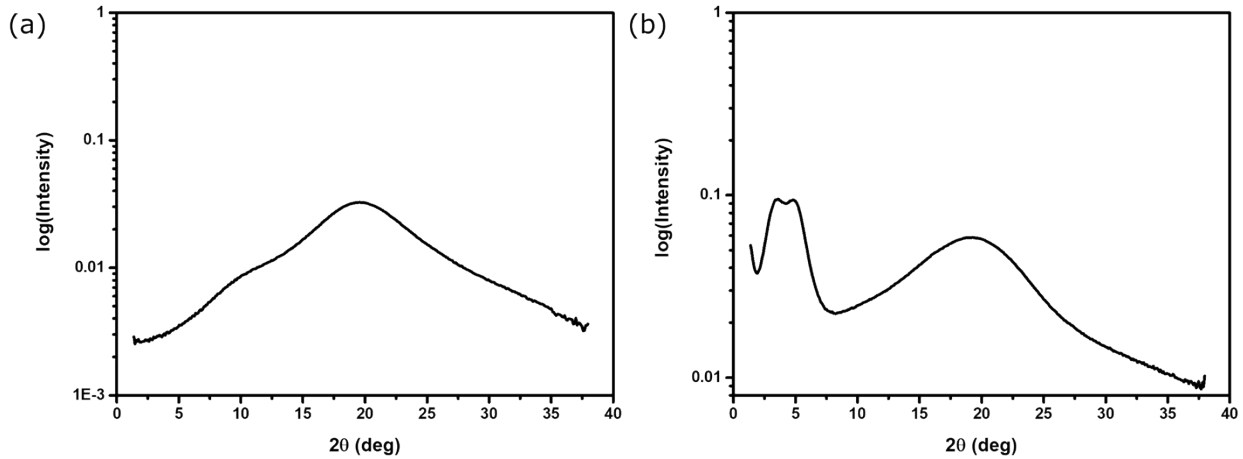

Figure S24. X-ray diffractograms of (a) a blank capillary tube and (b) **dDBP(6,6)** at 325 °C (isotropic phase).

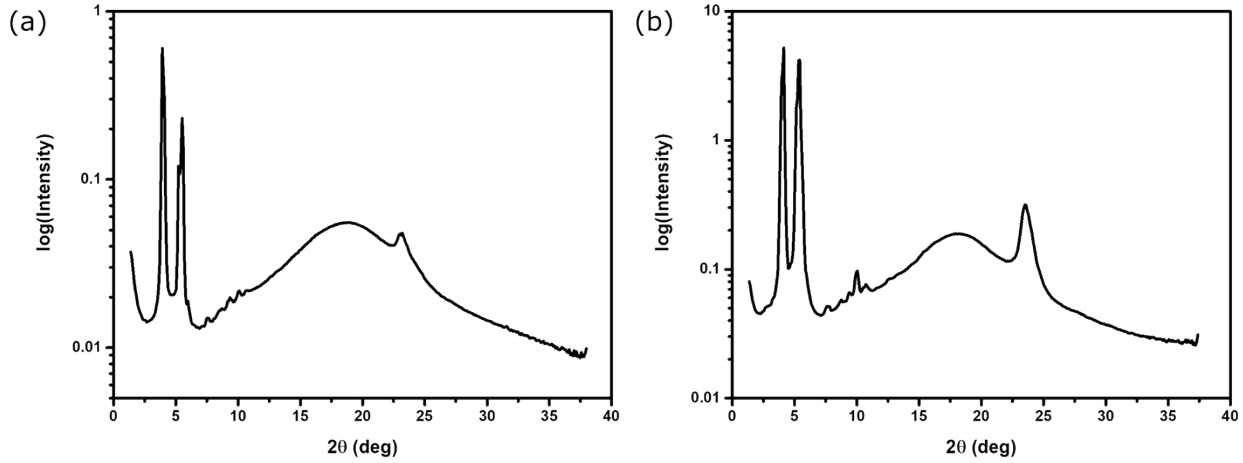

Figure S25. X-ray diffractograms of **dDBP(6,6)** at (a) 190 °C and (b) room temperature on cooling.

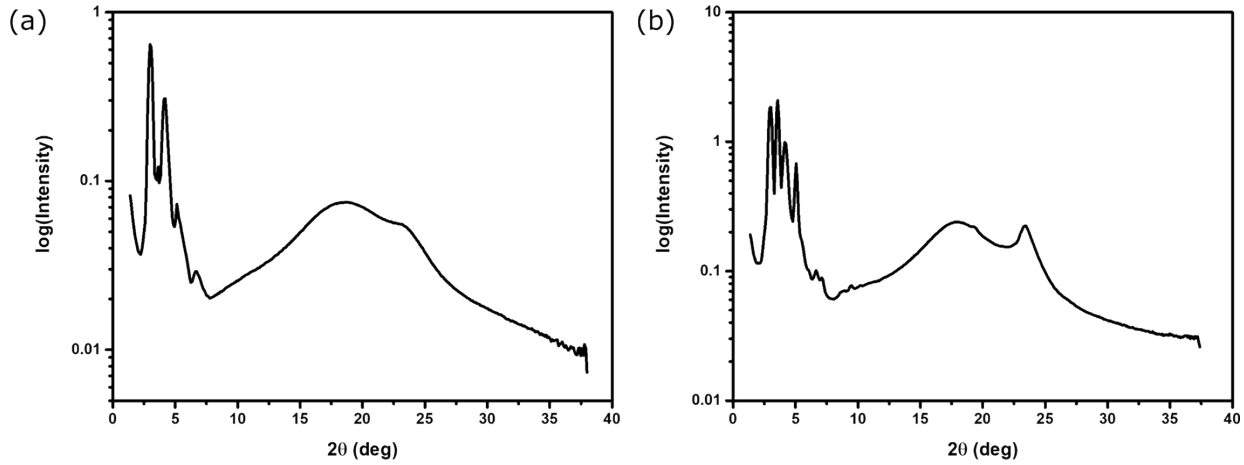

Figure S26. X-ray diffractograms of **dDBP(6,10)** at (a) 131 °C and (b) room temperature on cooling.

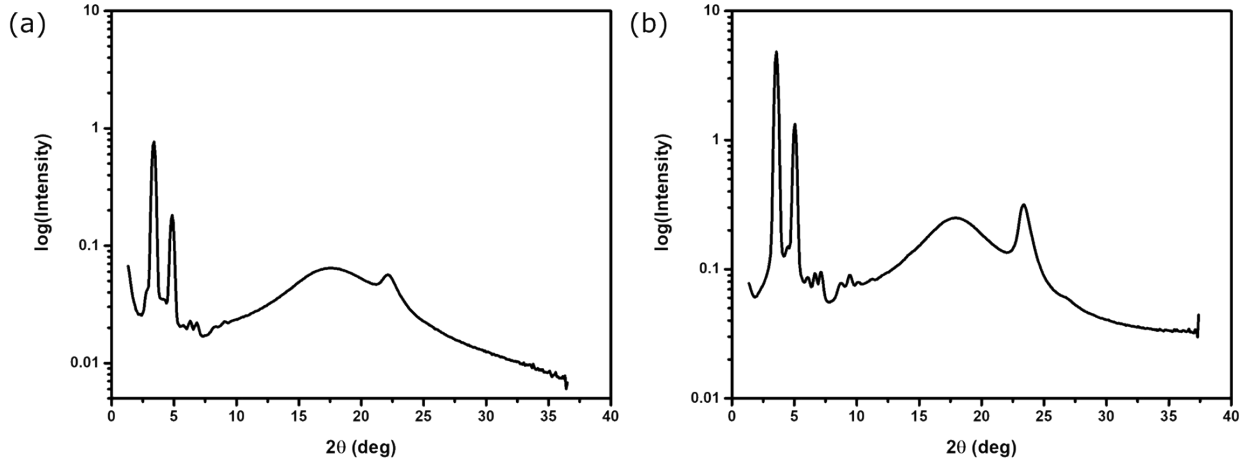

Figure S27. X-ray diffractograms of **dDBP(10,6)** at (a) 137 °C and (b) room temperature on cooling.

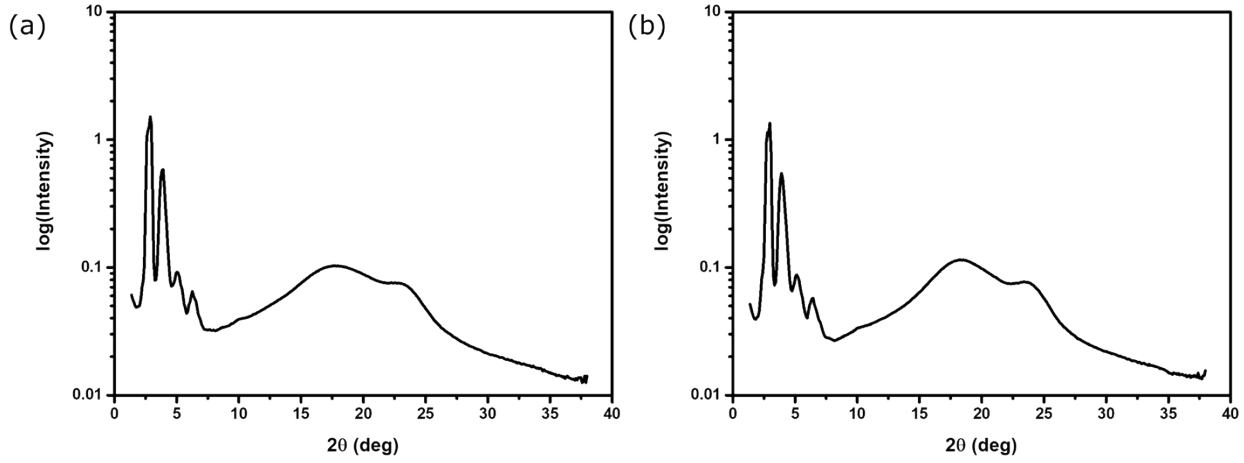

Figure S28. X-ray diffractograms of **dDBP(10,10)** at (a) 154 °C and (b) room temperature on cooling.

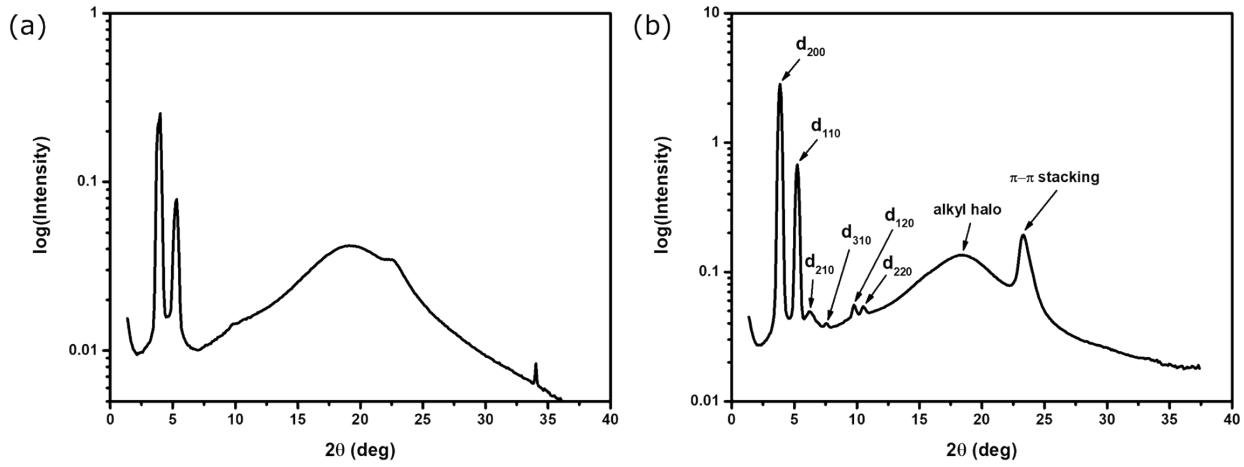

Figure S29. X-ray diffractograms of **dDBP-OHx(6,6)** at (a) 190 °C and (b) room temperature on cooling.

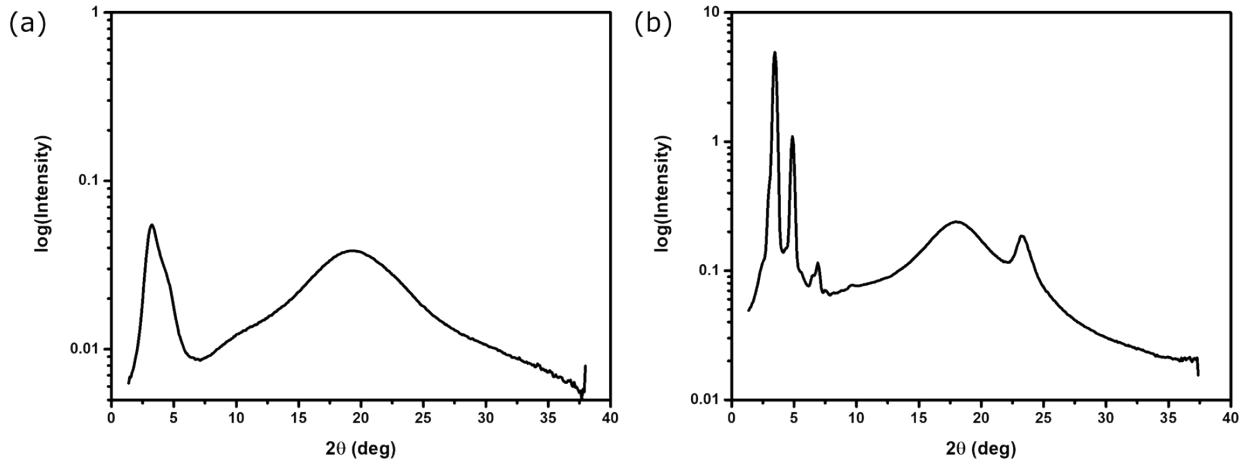

Figure S30. X-ray diffractograms of **dDBP-OHx(6,10)** at (a) 150 °C and (b) room temperature on cooling.

Table S1. X-ray diffraction data of the low temperature Col_r phase of **dDBP-OHx(6,6)**.

Compound	T (°C)	Miller Index (hkl)	d_{obs} (Å)	d_{calc} (Å)	Phase (lattice constants)
dDBP-OHx(6,6)	25	(200)	22.9	22.9	Col_r
		(110)	16.8	16.8	
		(210)	14.1	14.2	(a = 45.8 Å)
		(310)	11.7	11.7	(b = 18.1 Å)
		(120)	9.0	8.9	
		(220)	8.4	8.4	
		alkyl halo	4.8	N/A	
		π-π stacking	3.8	N/A	

Note: Col_r = columnar rectangular soft crystalline or plastic phase.

Table S2. X-ray diffraction data of the N_D phase of **dDBP-OHx(6,10)**.

Compound	T (°C)	Miller Index (hkl)	d-spacing (Å)	Phase
dDBP-OHx(6,10)	150	Lateral disc-to-disc	27.48	N_D
		Planar disc-to-disc	4.53	

5. Modelling Details

Density functional theory (DFT)[4] calculations were performed on truncated models of the compounds discussed in the manuscript (*i.e.*, the peripheral chains were shortened to methoxy groups). The calculations were performed using the B3LYP functional[5,6] at the 6-31G(d) level[7,8] with a Grimme D3[9,10] dispersion correction (B3LYP-D3). All calculations were performed using Gaussian 09.[11]

Two models were constructed to represent the direct ester series: one without (**dDBP(1,1)**) and one with (**dDBP-OMe(1,1)**) an adjacent methoxy group. For both models, different conformations were constructed depending on the dihedral angles between the ester linker and the DBP core. On the carbonyl end of the dimer, the carbonyl tends to orient planar to the DBP core; hence, only two dihedral angles were investigated on this end (**0** and **180** degrees). This is consistent with our previous investigations of DBP diesters.[12] On the end bound to the oxygen of the ester, five dihedral angles were tested for the ester: **0**, **45**, **90**, **135**, and **180** degrees. Overall, this gives ten conformations for both models (for **dDBP-OMe(1,1)**, the *ortho* methoxy group tends to orient planar to the DBP core, pointing away from the ester, as observed in Figure S31). All conformers are shown in Figures S32-S33 and their energies are summarized in Tables S3-S4. The lowest energy conformers for both models are shown in Figure S31.

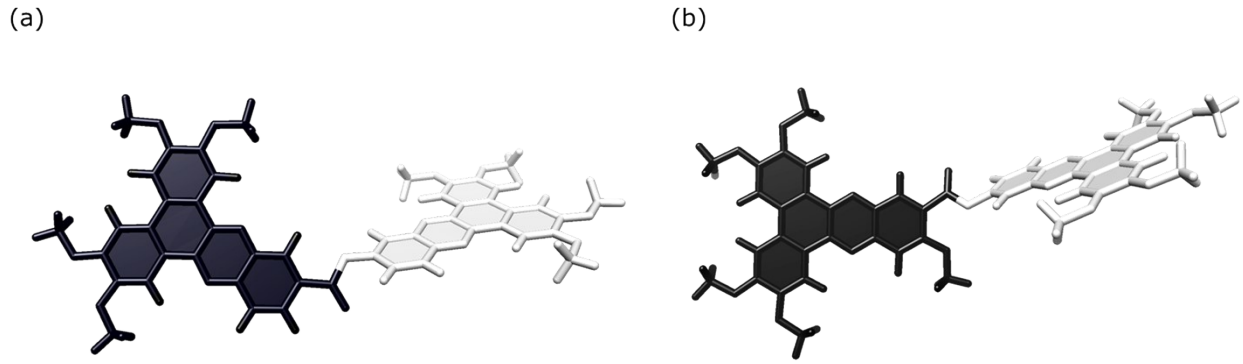

Figure S31. Lowest energy conformations for models (a) **dDBP(1,1)** and (b) **dDBP-OMe(1,1)**.

Table S3. Optimized conformations investigated for model compound **dDBP(1,1)**. The relative energy is proportionate to the lowest energy conformer.

Conformation	Input Dihedral Angles (deg)	Output Dihedral Angles (deg)	Energy (a.u.)	Relative Energy (kcal/mol)	Number of Imaginary Frequencies
1	(0, 0)	(0, 6)	-2861.4568	+0.57	0
2	(0, 45)	(1, 39)	-2861.4571	+0.38	0
3	(0, 90)	(0, 134)	-2861.4572	+0.32	0
4	(0, 135)	(0, 134)	-2861.4572	+0.32	0
5	(0, 180)	(0, 134)	-2861.4572	+0.32	0
6	(180, 0)	(180, 33)	-2861.4574	+0.14	0
7	(180, 45)	(180, 33)	-2861.4574	+0.14	0
8	(180, 90)	(178, 130)	-2861.4577	0	0
9	(180, 135)	(178, 130)	-2861.4577	0	0
10	(180, 180)	(178, 130)	-2861.4577	0	0

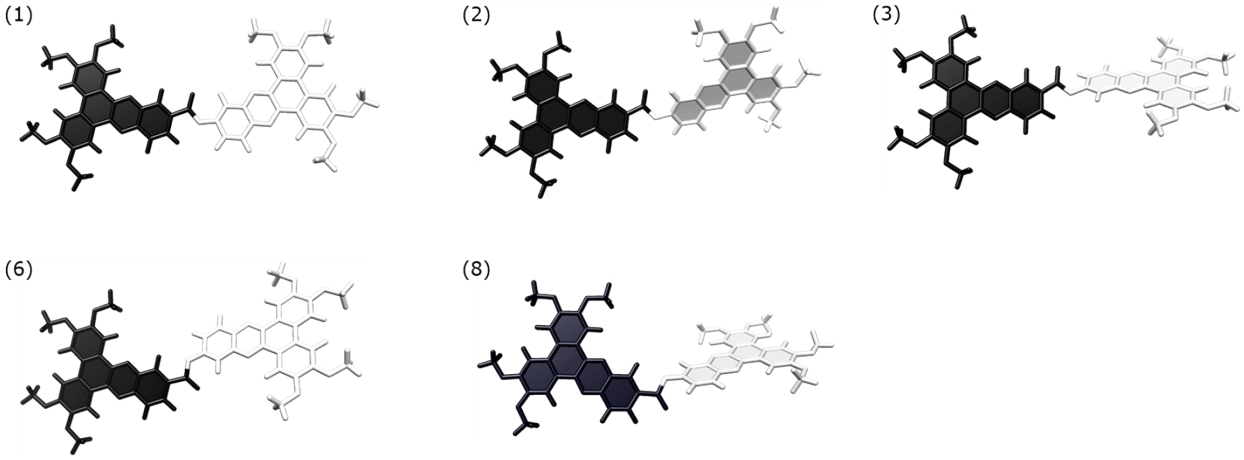

Figure S32. All five degenerate conformations optimized for **dDBP(1,1)**. The number in the figure corresponds to the conformation number in Table S3.

Table S4. Optimized conformations investigated for model compound **dDBP-OMe(1,1)**. The relative energy is proportionate to the lowest energy conformer.

Conformation	Input Dihedral Angles (deg)	Output Dihedral Angles (deg)	Energy (a.u.)	Relative Energy (kcal/mol)	Number of Imaginary Frequencies
1	(0, 0)	(27, 32)	-2975.9784	+0.03	0
2	(0, 45)	(27, 32)	-2975.9784	+0.03	1
3	(0, 90)	(23, 136)	-2975.9784	0	0
4	(0, 135)	(23, 136)	-2975.9784	0	0
5	(0, 180)	(23, 136)	-2975.9784	0	0
6	(180, 0)	(152, 9)	-2975.9775	+0.61	0
7	(180, 45)	(156, 40)	-2975.9778	+0.41	0
8	(180, 90)	(157, 130)	-2975.9779	+0.33	0
9	(180, 135)	(157, 130)	-2975.9779	+0.33	0
10	(180, 180)	(157, 130)	-2975.9779	+0.33	0

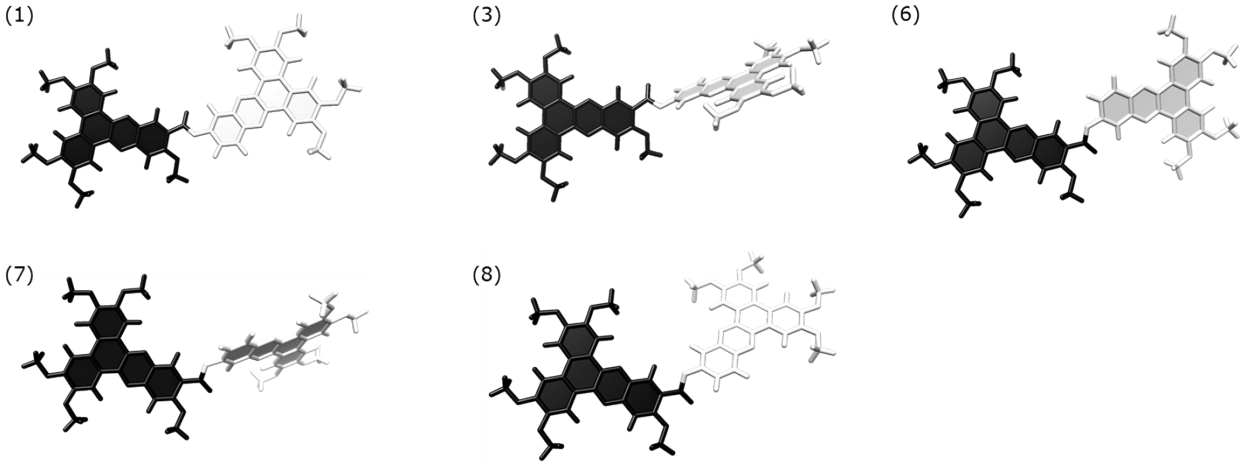

Figure S33. All five degenerate conformations optimized for **dDBP-OMe(1,1)**. The number in the figure corresponds to the conformation number in Table S4.

6. Cartesian Coordinates

dDBP(1,1) – lowest energy conformation

```
Charge =  0 Multiplicity = 1
 C                    -6.58185  -1.11187  -0.35995
 C                    -4.71944  -2.40669  -0.71672
 C                    -3.90038  -1.39792  -0.11125
 C                    -5.75634  -0.09821   0.25867
 H                    -4.74838  -4.34713  -1.65699
 C                    -4.10899  -3.59575  -1.20412
 C                    -2.50029  -1.59869  -0.01753
 C                    -1.93528  -2.76257  -0.50273
 C                    -2.75277  -3.76918  -1.09812
 H                    -1.89729  -0.82214   0.43782
 H                    -2.26902  -4.66831  -1.46415
 C                    -8.01686  -0.89801  -0.47529
 C                    -8.60013   0.29003   0.01703
 C                    -8.82     -1.88598  -1.08653
 C                    -9.99747   0.44492  -0.12828
 C                    -10.18399  -1.72053  -1.22028
 H                    -8.32306  -2.77685  -1.44703
 C                    -10.7848  -0.52454  -0.729
 H                    -10.47597   1.34309   0.23524
 C                    -6.37139   1.11947   0.77058
 C                    -5.5637    2.10126   1.38411
 C                    -7.76412   1.31403   0.65411
 C                    -6.10724   3.26834   1.88348
 H                    -4.50208   1.90275   1.44814
 C                    -8.30585   2.51433   1.16861
 C                    -7.51276   3.47791   1.77079
 H                    -9.36901   2.69465   1.0969
 N                    -4.44295  -0.25558   0.37017
 N                    -6.0552   -2.23877  -0.82993
 O                    -11.03692  -2.61086  -1.79243
 O                    -12.12905  -0.43992  -0.90175
 O                    -7.96522   4.65086   2.28547
 O                    -5.41343   4.26704   2.49043
 C                    -10.48524  -3.8171   -2.30018
 H                    -9.75218  -3.62153  -3.09438
 H                    -10.00532  -4.40579  -1.50676
 H                    -11.32625  -4.37827  -2.71138
 C                    -12.7953   0.72463  -0.44029
 H                    -13.84975   0.57846  -0.68081
 H                    -12.68363   0.84986   0.64553
 H                    -12.42789   1.62724  -0.94771
 C                    -9.35405   4.92866   2.20793
 H                    -9.69987   4.97094   1.16583
 H                    -9.94656   4.18226   2.75485
 H                    -9.48777   5.90699   2.67286
```

C	-4.00927	4.10314	2.62829
H	-3.51624	4.0154	1.65076
H	-3.65389	5.00179	3.13563
H	-3.76443	3.21991	3.23349
C	-0.47435	-3.0268	-0.43682
O	0.06213	-4.042	-0.82233
O	0.20461	-1.96907	0.1116
C	2.20829	-3.1153	0.92785
C	3.56794	-3.10507	1.11794
C	4.35705	-2.01891	0.64845
C	3.71429	-0.92782	-0.02492
C	2.30775	-0.95822	-0.21436
C	1.58935	-2.02996	0.25125
H	1.59861	-3.94033	1.27411
H	4.07393	-3.91899	1.6274
H	1.81855	-0.13505	-0.72291
C	5.74518	0.10837	-0.2924
C	6.39208	-0.98932	0.38491
C	7.83683	-0.96927	0.57435
C	8.60097	0.11666	0.09617
C	8.4663	-2.0449	1.23727
C	9.99905	0.08065	0.30628
C	9.83272	-2.06611	1.43471
H	7.83478	-2.85236	1.58318
C	10.61604	-0.97573	0.95634
H	10.61299	0.89691	-0.04732
C	6.54443	1.22492	-0.7801
C	7.94346	1.23247	-0.59311
C	5.90916	2.29763	-1.44263
C	8.6675	2.34053	-1.0909
C	6.62965	3.37341	-1.92197
H	4.83514	2.24188	-1.56044
C	8.04333	3.39238	-1.74154
H	9.74034	2.37687	-0.96551
N	4.42931	0.12324	-0.48314
N	5.69354	-2.02445	0.84152
O	11.95136	-1.07603	1.19092
O	10.52592	-3.05572	2.05932
O	8.67628	4.48494	-2.24508
O	6.10746	4.44949	-2.5698
C	10.08528	4.56772	-2.10772
H	10.37548	5.5078	-2.58037
H	10.38851	4.5832	-1.05161
H	10.5904	3.73429	-2.6154
C	4.70259	4.47517	-2.7734
H	4.36864	3.62801	-3.38768
H	4.15705	4.46246	-1.82006
H	4.49537	5.40929	-3.29876
C	12.79355	-0.03002	0.73579
H	12.53935	0.92892	1.2085
H	13.8065	-0.31697	1.02384
H	12.74416	0.08252	-0.35621

```
 C                     9.78845  -4.16533   2.54996
 H                     9.05426  -3.85818   3.30708
 H                     9.26721  -4.69294   1.73974
 H                     10.52283  -4.83245   3.00511
```

dDBP-OMe(1,1) – lowest energy conformation

```
Charge =  0 Multiplicity = 1
 C                    -6.55898  -0.54258  -0.59604
 C                    -4.37972  -0.66698  -1.30717
 C                    -4.09254   0.55967  -0.6288
 C                    -6.26771   0.69874   0.08263
 H                    -3.62012  -2.23404  -2.54972
 C                    -3.35088  -1.32471  -2.02796
 C                    -2.7735    1.07097  -0.67942
 C                    -1.7658    0.40994  -1.35163
 C                    -2.07011  -0.80777  -2.06501
 H                    -2.55294   1.99833  -0.16258
 C                    -7.90525  -1.09251  -0.53687
 C                    -8.91995  -0.41556   0.17491
 C                    -8.18831  -2.30964  -1.19546
 C                    -10.20722  -0.99949   0.19801
 C                    -9.45039  -2.86749  -1.16291
 H                    -7.375    -2.78658  -1.72604
 C                    -10.48367  -2.19375  -0.44826
 H                    -11.00627  -0.50745   0.73404
 C                    -7.32333   1.39055   0.81125
 C                    -7.03436   2.60582   1.46831
 C                    -8.62498   0.84829   0.85906
 C                    -8.00668   3.29195   2.16936
 H                    -6.02096   2.97886   1.40129
 C                    -9.60973   1.56196   1.58067
 C                    -9.32564   2.75461   2.22578
 H                    -10.61718   1.17451   1.63588
 N                    -5.04772   1.22441   0.05604
 N                    -5.62149  -1.19915  -1.27594
 O                    -9.81677  -4.03189  -1.76311
 O                    -11.69489  -2.80844  -0.46641
 O                    -10.22132   3.49081   2.9356
 O                    -7.82338   4.46529   2.83073
 C                    -8.82102  -4.73832  -2.48721
 H                    -8.42717  -4.13948  -3.31967
 H                    -7.98783  -5.03952  -1.83773
 H                    -9.31506  -5.62836  -2.88125
 C                    -12.77197  -2.19367   0.22231
 H                    -13.63204  -2.84902   0.07405
 H                    -12.56477  -2.10319   1.29753
 H                    -12.99749  -1.19921  -0.18682
 C                    -11.55297   3.01371   3.03473
```

H	-12.0304	2.93976	2.04768
H	-11.5951	2.03346	3.52963
H	-12.08771	3.74751	3.64046
C	-6.52497	5.0408	2.80118
H	-6.21245	5.27663	1.77508
H	-6.59559	5.9627	3.38119
H	-5.77962	4.37645	3.2587
C	-0.41595	1.04331	-1.26545
O	-0.23762	2.21895	-1.03173
O	0.59376	0.13713	-1.40434
C	2.39764	1.65686	-2.09101
C	3.73555	1.96441	-2.06661
C	4.64876	1.17728	-1.31224
C	4.15479	0.04843	-0.57799
C	2.76816	-0.25051	-0.61086
C	1.92307	0.54228	-1.34632
H	1.6959	2.25504	-2.65747
H	4.13006	2.81064	-2.62021
H	2.39139	-1.10403	-0.05863
C	6.28233	-0.41196	0.15087
C	6.77836	0.72714	-0.58239
C	8.19955	1.04765	-0.54217
C	9.08795	0.24534	0.2055
C	8.68052	2.16769	-1.25432
C	10.45548	0.60592	0.21038
C	10.01877	2.50741	-1.23969
H	7.95784	2.74964	-1.81079
C	10.92629	1.70523	-0.48869
H	11.16181	0.01379	0.77478
C	7.20984	-1.23486	0.91648
C	8.58482	-0.91764	0.94488
C	6.72237	-2.35234	1.62842
C	9.43729	-1.75373	1.70275
C	7.56716	-3.1591	2.36432
H	5.66015	-2.55052	1.57361
C	8.95802	-2.85036	2.40046
H	10.4958	-1.53963	1.74471
N	4.99147	-0.73082	0.1424
N	5.96113	1.49472	-1.2975
O	12.22403	2.10934	-0.52732
O	10.57348	3.56535	-1.89025
O	9.71892	-3.69444	3.14688
O	7.19156	-4.25318	3.0802
C	11.11226	-3.44537	3.231
H	11.51655	-4.23001	3.8731
H	11.59315	-3.4996	2.24437
H	11.32128	-2.46444	3.68005
C	5.81469	-4.59928	3.07651
H	5.1959	-3.79644	3.49967
H	5.45903	-4.82788	2.06264
H	5.73064	-5.49073	3.70089
C	13.18261	1.35905	0.19967

H	13.23985	0.32146	-0.15777
H	14.14038	1.85352	0.02756
H	12.96291	1.35726	1.27642
C	9.70725	4.40091	-2.64347
H	9.21326	3.84534	-3.45214
H	8.94044	4.86378	-2.00767
H	10.34256	5.17835	-3.07188
O	-1.05658	-1.35934	-2.77383
C	-1.30681	-2.55299	-3.50309
H	-1.61424	-3.37077	-2.83839
H	-2.07716	-2.4006	-4.27055
H	-0.3598	-2.80822	-3.98109

7. References

(1) Foster, E. J.; Babuin, J.; Nguyen, N.; Williams, V. E. Synthesis of Unsymmetrical Dibenzoquinoxaline Discotic Mesogens. *Chem. Commun.* **2004**, *10* (18), 2052–2053.

(2) Zellman, C. O.; Vu, D.; Williams, V. E. Adjacent Functional Group Effects on the Assembly of Columnar Liquid Crystals. *Can. J. Chem.* **2020**, *98* (7), 379–385.

(3) Foster, J. E.; Lavigueur, C.; Ke, Y.-C.; Williams, V. E. Self-Assembly of Hydrogen-Bonded Molecules: Discotic and Elliptical Mesogens. *J. Mater. Chem.* **2005**, *15* (37), 4062–4068.

(4) Parr, R. G.; Yang, W. Y. Density-functional theory. In *Density Functional Theory of Atoms and Molecules*; Oxford University Press: New York, 1989; pp 47-69.

(5) Lee, C.; Yang, W.; Parr, R. G. Development of the Colle-Salvetti Correlation-Energy Formula into a Functional of the Electron Density. *Phys. Rev. B* **1988**, *37* (2), 785–789.

(6) Becke, A. D. Density-Functional Thermochemistry. III. The Role of Exact Exchange. *J. Chem. Phys.* **1993**, *98* (7), 5648–5652.

(7) Francl, M. M.; Pietro, W. J.; Hehre, W. J.; Binkley, J. S.; Gordon, M. S.; DeFrees, D. J.; Pople, J. A. Self-Consistent Molecular Orbital Methods. XXIII. A Polarization-Type Basis Set for Second-Row Elements. *J. Chem. Phys.* **1982**, *77* (7), 3654–3665.

(8) Hill, J. G. Gaussian Basis Sets for Molecular Applications. *Quantum Chem.* **2013**, *113* (1), 21–34.

(9) Grimme, S. Accurate Description of van Der Waals Complexes by Density Functional Theory Including Empirical Corrections. *J. Comput. Chem.* **2004**, *25* (12), 1463–1473.

(10) Grimme, S.; Antony, J.; Ehrlich, S.; Krieg, H. A Consistent and Accurate *ab initio* Parametrization of Density Functional Dispersion Correction (DFT-D) for the 94 Elements H-Pu. *J. Chem. Phys.* **2010**, *132* (15), 154104.

(11) Frisch, M. J.; Trucks, G. W.; Schlegel, H. B.; Scuseria, G. E.; Robb, M. A.; Cheeseman, J. R.; Scalmani, G.; Barone, V.; Petersson, G. A.; Nakatsuji, H.; Li, X.; Caricato, M.; Marenich, A.; Bloino, J.; Janesko, B. G.; Gomperts, R.; Mennucci, B.; Hratchian, H. P.; Ortiz, J. V.; Izmaylov, A. F.; Sonnenberg, J. L.; Williams-Young, D.; Ding, F.; Lipparini, F.; Egidi, F.; Goings, J.; Peng, B.; Petrone, A.; Henderson, T.; Ranasinghe, D.; Zakrzewski, V. G.; Gao, J.; Rega, N.; Zheng, G.; Liang, W.; Hada, M.; Ehara, M.; Toyota, K.; Fukuda, R.; Hasegawa, J.; Ishida, M.; Nakajima, T.; Honda, Y.; Kitao, O.; Nakai, H.; Vreven, T.; Throssell, K.; Montgomery Jr., J. A.; Peralta, J. E.; Ogliaro, F.; Bearpark, M.; Heyd, J. J.; Brothers, E.; Kudin, K. N.; Staroverov, V. N.; Keith, T.; Kobayashi, R.; Normand, J.; Raghavachari, K.; Rendell, A.; Burant, J. C.; Iyengar, S. S.; Tomasi, J.; Cossi, M.; Millam, J. M.; Klene, M.; Adamo, C.; Cammi, R.; Ochterski, J. W.; Martin, R. L.; Morokuma, K.; Farkas, O.; Foresman, J. B.; Fox, D. J. Guassian 09. Gaussian, Inc.: Wallingford CT 2016.

(12) Zellman, C. O.; Williams, V. E. Stereochemistry, Conformational Dynamics, and the Stability of Liquid Crystal Phases. *J. Org. Chem.* **2021**, *86* (21), 15076–15084.